Characterization of Major N-linked Sugar Chain Structures Expressed in Mouse Cerebral Cortex during Development

Takeshi Ikeda

Doctor of Philosophy

Department of Physiological Sciences, School of Life Sciences, The Graduate University for Advanced Studies

and

Laboratory of Neural Information, National Institute for Physiological Sciences, Okazaki National Research Institutes

2002

Table of Contents

Abstract

The expression pattern of numerous N-linked sugar chains including those preferentially expressed in the brain are spatiotemporally regulated in the central nervous system (CNS) during development with little variation among individuals, which are indispensable for normal development. However, precise structure of each sugar chain has not been determined yet. Understanding of the structure of the sugar chains expressed in the CNS during development would be crucial in elucidating the physiological significances of the N-linked sugar chains in the brain.

In the present study, I analyzed the expression pattern of major N-linked sugar chains in the mouse cerebral cortex during development by two-dimensional HPLC following pyridylamination of the sugar chains released by hydrazinolysis. I determined their structure, using a combination of matrix-assisted laser-desorption ionization time-of-flight mass spectrometer (MALDI/TOF-MAS) and exoglycosidase digestion followed by two-dimensional HPLC mapping.

One sugar chain structure I determined, A2G1Fo(6)G'1(3)F, was a novel structure that has not been reported to be expressed in the brain. During development, the amount of M5A increased steadily and became most abundant in the oligomannose series. In the complex and hybrid type N-linked sugar chains, typical brain-type structural features such as outer-arm α1-3 fucosylation, α1-6 core fucosylation, a bisecting N-acetylglucosamine (GlcNAc) residue, non-reducing terminals lacking galactose (Gal) residue, absence of the GlcNAc residue on the α1-3 mannose branch and Gal residues linked via β1-3 linkage to GlcNAc were prominent in 12 weeks old mouse.

Neurogenesis followed by neuronal migration occurs from embryonic day 12 to 16 in mouse cerebral cortex. During this period β1-4Gal-T-Ⅰ gene expression is

dramatically down regulated followed by the reduction of the N-linked sugar chains containing β1-4Gal residues on the non-reducing ends, resulting in an increase of such sugar chains containing GlcNAc residues on the non-reducing ends afterwards. When the neurogenesis subsides and the production of astrocyte starts at embryonic day 16, the expression of typical brain-type structural elements such as bisecting GlcNAc, core Fuc and LewisX epitopes gradually increased. When the production of oligodendrocyte starts after birth, the expression of the N-linked sugar chains containing Gal residues connected via β1-3 linkages appeared. When the production of astrocyte subsides and synaptogenesis occurs followed by onset of myelination at postnatal day 7, the expression of the sugar chains containing no GlcNAc residue on the α1-3 Man branch appeared and the amount of sugar chains containing bisecting GlcNAc, core Fuc and LewisX epitopes reached their maximum. These results suggest that each of these brain-type sugar chains has its own distinct role in the brain.

Abbreviations

The nomenclature of oligosaccharide structure is as follows: An (where n = 0-2) indicates the number of antennae linked to the trimannosyl core; Gn (where n = 0-2), the number of galactose residues attached via β1-4 linkage to the non-reducing ends; G'n (where n = 1-2), the number of galactose residues attached via β1-3 linkage to the non-reducing ends; F, with core fucosylation; Fo, with outer arm fucosylation attached via α1-3 linkage to N-acetylglucosamine residues; B, with bisecting N-acetylglucosamine residues.

The isobaric monosaccharide composition: H = hexose, N = N-acetylhexosamine, F = Fuc.

GlcNAc:	N-acetylglucosamine
Man:	mannose
Gal:	galactose
Fuc:	fucose
Fuc-T:	fucosyltransferase
Gn-T:	N-acetylglucosaminyltransferase
Gal-T:	β1-4galactosyltransferase
β-Hexase:	N-acetyl-β-D-hexosaminidase
E12:	embryonic day 12
E16:	embryonic day 16
P0:	postnatal day 0
P7:	postnatal day 7
12W:	12 weeks

21W:	21 weeks
GU:	glucose unit
MU:	mannose unit
CNS:	central nervous system
ER:	endoplasmic reticulum
HPLC:	high performance liquid chromatography
MALDI/TOF-MAS:	matrix-assisted laser-desorption ionization time-of-flight mass spectrometer
PCR:	polymerase chain reaction
RA:	relative abundance
RT-PCR:	reverse transcriptase-PCR
SSEA-1	stage specific embryonic antigen-1
SVZ:	subventricular zone
PA-:	pyridylamino

Introduction

Physiological significances of N-linked sugar chains expressed on glycoproteins in the central nervous system during development

N-linked sugar chains on glycoproteins, which envelop a vast majority of the cell surface, are considered to play pivotal roles in cell-to-cell and extracellular matrix interactions. Intracellularly N-linked sugar chains play a common role in promoting protein folding, quality control and certain sorting events (Helenius and Aebi 2001). It is considered that the processing of N-linked sugar chains in the ER and Golgi of all mammalian cells from any species or tissues follow the same principal metabolic pathways, but analyses have revealed that the structure of N-linked sugar chains of a glycoprotein may be dependent on the tissue in which it is expressed (Parekh et al. 1987). The sugar chains expressed in the brain are consisted of a variety of hybrid and complex type structures including structural features that are not commonly found in other organs (Shimizu et al. 1993; Chen et al., 1998; Zamze et al., 1998).

The research group of Hase (Hase et al. 1981; 1987; 1988) and Ikenaka (Fujimoto et al. 1999; Otake et al. 2001), has recently developed a systematic method to analyze N-linked sugar chain expression pattern present in a whole tissue without purification of glycoproteins. Using this method, they showed that the expression patterns are strictly regulated so that there were little differences among individuals when identical regions of age-matched brain were analyzed (Fujimoto et al., 1999). This result was unexpected because the structures of N-linked sugar chains from a purified glycoprotein showed diverse heterogeneity. For examples, human blood clotting factor Ⅸ (Factor Ⅸ, Christmas factor) has two N-glycosylation sites (Kurachi and Davie 1982), but there are eight major N-linked sugar chains without taking sialylation into considerations (Makino et al. 2000).

While the expression pattern of sugar chains in the CNS are constant with very little variation, they dramatically change during development (Trenkner and Sarkar 1977; Nakakita et al. 1998; Yoshimi et al. 1999). N-linked sugar chains have been demonstrated to be essential for normal development and maintenance of CNS by the genetic modifications of the N-glycosylation enzymes in mice (Furukawa et al. 2001; Ioffe and Stanley 1994; Metzler et al. 1994). But their physiological functions in the CNS during development are poorly understood. It is partly because the genetically modified mice often die during the development, and the detailed analyses of the sugar chains expressed during the development have not been done. The changes in the expression level of N-linked sugar chains which are predominantly found in the brain during development may be involved in the processes of differentiation, migration and maturation of neural cells. Accordingly, the analysis of these brain-type sugar chain expression pattern in the CNS during development would be critical in elucidating the physiological significance of N-linked sugar chains during development. I focused on cerebral cortex as a model of CNS development and performed comprehensive analysis of the major N-linked sugar chains expressed in whole tissues.

The development of cerebral cortex in mice

The structure of mammalian cerebral cortex is highly ordered consisting of various kinds of cells including neurons and glial cells. The neurogenesis commences around embryonic day 11 (E11) and continues until about E16 or E17 (Jacobson, M. 1991). On the other hand, cortical astrocytes are first detected around E16 and oligodendrocytes around birth, but the vast majority of both cell types are produced during the first postnatal month (Sauvageot and Stiles 2002).

Different classes of neuron lie in radially organized array consisting of six cellular

layers piling up from white matter to the pial surface in the cerebral cortex. These layers are normally formed through the inside-out pattern, with later-born neurons migrating past older ones to form progressively superficial, and thus younger, layers of the cortex. The formation of these laminated structures is a remarkably complex process, and mainly consists of two distinct steps (Sun et al. 2002). First, in about E11, the earliest-born cortical neurons including the Cajal-Retzius and prospective subplate neurons form the preplate, a layer of differentiated neurons superficial to the proliferative cells of the ventricular zone. Second, subsequently generated postmitotic neurons migrate radially along the glial fibers into the preplate and intercalate between the inner and outer cell populations, to form the cortical plate from E12 to E17 (Allendoerfer and Shatz 1994).

Cortical astrocytes are considered to originate from two sources. First, astrocytes develop from precursor cells that emerge from the dorsolateral subventricular zone (SVZ) to colonize adjacent gray and white matter between E16 and the first postnatal days (Levison and Goldman 1993; Luskin and McDermott 1994). Second, astrocytes differentiate from radial glia between P0 and P10, themselves established from the neuroepithelium earlier in development around the time of neurogenesis and neuronal migration (Luskin et al. 1988; Price and Thurlow 1988; Voigt, T. 1989). Most of cortical oligodendrocytes are considered to originate from localized regions of the ventral neuroepithelium (first appear in around E11) and populate more dorsal regions, the developing cerebral cortex, by long-range cell migration and proliferation during embryogenesis (Woodruff et al. 2001).

During the first postnatal week, the ventricular zone is depleted of cells and disappear, the intermediate zone transforms into the white matter and the cortical plate becomes laminated (Bayer and Altman 1991). By the end of the first month, gliogenesis subsides and the cortex is mature in most respects (Bayer and Altman

1991).

Considering both neuronal and glial development in the cerebral cortex as described above, I chose the following five developmental stages of mice.

(1) At E12, the neurogenesis commences followed by neuronal migration.

(2) At E16, the neurogenesis subsides and the production of astrocyte starts.

(3) At P0, the production of oligodendrocyte starts.

(4) At P7, the production of astrocyte subsides and synaptogenesis occurs followed by onset of myelination.

(5) At 12W, the cortex is mature.

Methodological Concerns

The stage-dependent expression of a certain sugar chain has often been identified by immunohistochemical approach or by lectin staining. But there are no antibodies or lectins that recognize the whole structure of a N-linked sugar chain specifically. This means that one cannot see the whole structure of N-linked sugar chains but a part of them using these techniques. For example, the LewisX epitope, which is also known as CD15 or SSEA-1 (stage-specific embryonic antigen-1) has been identified as a glycan epitope with a Galβ1-4(Fucα1-3)GlcNAcβ1- structure (Gooi et al. 1981; Hakomori et al. 1981; Kobata and Ginsburg 1969). Though several immunohistochemical studies have demonstrated that the expression of LewisX epitope is spatiotemporally regulated in the CNS during development, the whole structure of the sugar chains detected were different depending on the antibodies, regions, age and species used for analysis. LewisX epitope could be expressed not only on N-linked sugar chain but also on O-linked sugar chains or on glycolipid, thus the epitope could be expressed on many sugar chain backbones.

Different from such approach as immunohistochemistry or lectin staining, one can

analyze not only the epitopes but the entire structure of sugar chains expressed in tissues by HPLC. Previously complete characterizations of neutral and sialylated N-linked sugar chains expressed in adult rat brain have been examined systematically (Chen et al. 1998; Zamze et al. 1998), furthermore, it has been shown that the profiles of their expressions are highly conserved among human, mouse and rat (Albach et al. 2001). But their method required many chromatographic steps for purification or separating sugar chains, making it unsuitable for analyzing a large number of samples or small amounts of samples. On the other hand, the previously developed method by the research group of Hase (Hase et al. 1981; 1987; 1988) and Ikenaka (Fujimoto et al. 1999; Otake et al. 2001) can analyze sugar chains expressed in whole tissues easily and reproducibly from amounts as low as 2 mg of acetone precipitated brain tissue (Fujimoto et al. 1999). Accordingly, I adopted this method for accomplishing the present investigation.

Therefore, in the present study, I analyzed and determined the structures of the major N-linked sugar chains expressed in the mouse cerebral cortex by HPLC following pyridylamination of sugar chains released by hydrazynolysis. I constructed precise two-dimensional map of pyridylaminated N-linked sugar chains expressed in adult mouse brain and determined their structures, using a combination of MALDI/TOF-MAS and exoglycosidase digestion followed by two-dimensional HPLC mapping (Fujimoto et al. 1999; Otake et al., 2001). Using this information, I determined the structures of the major sugar chains expressed in mouse cerebral cortex during development. The expression levels of the sugar chains predominantly found in the brain were low in the cerebral cortex of embryonic day 12 mouse, but they increased during development, and gradually became major component of N-linked sugar chains. However, their developmental profiles were not identical

among each brain-type sugar chain, suggesting their distinct functions.

Materials and Methods

Materials

Various standard PA-sugar chains were purchased from Takara (Japan) or Seikagaku Corporation (Japan). Gb-BA-2 (see Table 1) was prepared through partial digestion of the commercially available standard PA-sugar chain G2-BA-2 (see Table 1) by *Diplococcus pneumoniae* β-galactosidase.

Pyridylamination of sugar chains released from tissue samples

Adult ICR mice of 12 weeks old were sacrificed, their whole brains quickly removed and washed with ice-cold PBS(-). Tissues were homogenized with nine-fold volume of acetone using polytron homogenizer. After placing on ice for 1 hour, the homogenate was centrifuged at 2,150×g for 20 min. The pellet was dried in a spinvac centrifuge. ICR mice of various developmental stages (E12, E16, P0, P7) or adult (12W) were sacrificed their cerebral cortices quickly removed and processed as described above.

Hydrazinolysis and pyridylamino (PA) derivatization were performed (1) manually or (2) by the automated GlycoPrep^{TM} (Oxford Glycosystems, Oxford, UK) and GlycoTag^{TM} (Takara, Japan) (Fig. 1). All samples used for developmental changes in the sugar chain expression levels were manually hydrazynolyzed followed by N-acetylation, and pyridylaminated using the GlycoTag^{TM}.

(1) *Hydrazynolysis and N-acetylation:* A lyophilized sample (2 mg) was heated with 200 µl anhydrous hydrazine at 100°C for 10 h. Excess hydrazine was evaporated *in vacuo*. The remaining trace of hydrazine was removed by co-evaporation with toluene several times. The sugar chains released were N-acetylated with freshly prepared sodium bicarbonate solution (saturated, 200

μl) and acetic anhydride (8 μl) by incubation on ice. Five minutes later, another 200 μl of the bicarbonate solution and 8 μl of acetic anhydride were added. The reaction mixture was left to stand for 30 min on ice with occasional stirring. Dowex 50W-X2 (1 g, H^+ form, 100-200 mesh; Bio-Rad, Hercules, CA) was added to the solution to bring the pH to 3. The resin and the solution were poured into a Sepacol mini column™ (Seikagaku Corporation, Tokyo, Japan), and the column was washed with 5-fold bed volumes of distilled water. The flow-through fraction and the washings were combined and concentrated to dryness by a rotary evaporator. A small amount of distilled water was added to the residue and the solution was lyophilized in a conical tube (Takara, Japan). *Pyridydamination:* Sugar chains released from the glycoproteins were heated with 20 μl of a pyridylamination reagent (prepared by mixing 552 mg 2-aminopyridine and 200 μl acetic acid) at 90°C for 60 min. The Schiff base was reduced by heating with 70 μl of a reducing reagent (freshly prepared by mixing 200 mg dimethylamine-borane complex, 50 μl water, and 80 μl acetic acid) at 80°C for 35 min. The reaction mixture was added to 90 μl water followed by extraction twice with 90 μl water-saturated phenol:chloroform (1:1, v/v) and once with 90 μl chloroform. The aqueous phase was poured onto a small column of Dowex 50W-X8 (NH_4^+ form, 0.5 × 3 cm; Bio-Rad, Hercules, CA), which was washed with 2 ml of 20 mM ammonium acetate buffer, pH 8.5.

(2) *Hydrazynolysis and N-acetylation:* A lyophilized acetone precipitate (2 mg) was hydrazinolyzed and N-acetylated using the GlycoPrep™. The GlycoPrep was run in the N-linked mode for specifically processing the N-linked sugar chains from the tissue sample. The conditions used, such as temperature (95°C) and time (10 h), for the hydrazinolysis were determined according to the

manufacture's instructions. *Pyridydamination:* These samples were lyophilized and applied to the GlycoTag™ for pyridylamination. Excess reagents were removed by extraction twice with 100 µl water-saturated phenol:chloroform (1:1, v/v) followed by extraction with 100 µl chloroform and with 100 µl diethyl-ether.

After suspension of the lyophilized sample in 50 µl of distilled water, the sample was filtered using 0.2 µm low-binding hydrophilic PTFE membrane Ultrafree™ centrifugal filter (MILLIPORE, Japan) before injection into HPLC columns.

Sugar chain analysis by HPLC

To analyze the expression pattern of both the neutral backbone of the sialylated sugar chains and the unsialylated sugar chains, PA-sugar chains (< 200 pmol) were digested with excess units of neuraminidase (from Arthrobacter ureafaciens; Nacali Tesque, Kyoto, Japan) in 50 mM acetate buffer solution (pH 5.0) at 37 °C for 18 h (Fig. 1). Neutral sugar chains of varying size (in accordance to the number of sugars present on each chain) were separated using an Asahipak NH2P-50 column (4.6×50 mm; Shodex, Tokyo, Japan). Samples were size fractionated from M3 to M11 according to the mannose unit standards M3, M4B, M5A, M6B, M7A, M8A and M9A (PA-Sugar Chain 016, 058, 017, 018, 052, 019, 020, respectively; Takara, Japan) (Fig. 2 and see Table 1). The M10 and M11 elution time was settled as M9 elution time +1.2 and +2.4, respectively. Each fraction was subjected to reverse-phase HPLC on a Cosmosil 5C18-P column (4.6×150 mm; Nacali Tesque, Kyoto, Japan) (Fig. 2). Before applying the samples, PA-glucose oligomer (Takara, Japan), consisting of pyridylaminated isomaltooligosaccharides containing PA-labeled glucose trimer to 22-mer, was injected into the column as external standards of reverse-phase HPLC. The glucose unit (GU) value of each sample peak was calculated by comparing its

elution time with those of the two nearest peaks of glucose oligomers.

To analyze the sugar chain expression patterns of the sialylated and the neutral components separately, PA-sugar chains of varying negative charges (in accordance with the number of sialic acid residues present on each chain) were separated using a MonoQ HR5/5 column (5×50 mm; Amersham Biosciences, NJ, USA) (Fig. 1). PA-sugar chains were further purified with a Cellulose Cartridge Glycan preparation kit™ (Takara, Japan) to remove the N-acetylation and pyridylamination reagents completely according to the manufacture's instructions. The lyophilized PA-sugar chain samples were suspended in 400 μl of butanol/ethanol/0.6M acetic acid (4:1:1), and then applied to a cellulose cartridge column. After washing the column with 10 ml of butanol/ethanol/0.6M acetic acid (4:1:1), the PA-sugar chains were eluted from the column with 2 ml of ethanol/75mM NH_4HCO_3 (1:2). Following suspension of the lyophilized samples in a small volume of distilled water, an aliquot was subjected to ion exchange HPLC to detect acidic sugar chain pattern. Samples were fractionated into the non-, mono-, di-, tri- and tetra-sialylated components (N, S1-S4) according to the neutral or sialylated N-acetyllactosamine type, biantennary standards (PA-sugar chain 001, 021, 023, 024, 025; Takara, Japan) (see Fig. 9). The N fraction and the neuraminidase-digested S1-S4 fractions of MonoQ HPLC were also size fractionated and subjected to reverse-phase HPLC (Fig. 1).

PA-sugar chains were detected by scanning fluorescence detector (FP-2025; Jasco, Japan). Each HPLC step was performed as follows.

Size-fractionation HPLC was performed on an Asahipak NH2P-50 column at a flow rate of 0.6 ml/min at 30°C. Solvent A consisted of 93% acetonitrile, 0.3% acetic acid (pH 7.0), and solvent B consisted of 20% acetonitrile, 0.3% acetic acid (pH 7.0). The column was equilibrated with mixtures of solvents A and B (ratio 97:3). After injecting a sample, proportion of solvent B was increased linearly to 15% in 5 min, to

30% in 25 min, and then 70% in 5 min. PA-sugar chains were detected at an excitation wavelength of 310 nm and emission wavelength of 380 nm (Hase, 1994).

Reverse-phase HPLC was performed on a Cosmosil 5C18-P column at a flow rate of 1.5 ml/min at 30°C. Solvent C consisted of 3.77 mM ammonium acetate buffer (pH 4.0), and solvent D was composed of solvent C containing 0.5% 1-butanol. The column was equilibrated with a mixture of solvent C and D at a 94:6 ratio. After injecting a sample, proportion of solvent D was increased linearly to 80% in 45 min. PA-sugar chains were detected at an excitation wavelength of 320 nm and emission wavelength of 400 nm.

Reverse-phase HPLC using a ShimPak CLC-ODS column (0.6×150 mm; Shimadzu, Kyoto, Japan) was performed at a flow rate of 1.0 ml/min at 55°C as reported (Tomiya et al., 1988). Solvent E consisted of 10 mM phosphate buffer (pH 3.8), and solvent F composed of solvent E containing 0.5% 1-butanol. The column was equilibrated with a mixture of solvent E and F at an 80:20 ratio. After injecting a sample, proportion of solvent F was increased linearly to 50% in 60 min. PA-sugar chains were detected at an excitation wavelength of 320 nm and emission wavelength of 400 nm.

Mono Q HPLC was performed on a Mono Q HR5/5 column at a flow rate of 1.0 ml/min at 25°C. Solvent G consisted of distilled H_2O titrated to pH 9.0 with 1 M aqueous ammonia, and solvent H consisted of 0.5 M ammonium acetate (pH 9.0). The column was equilibrated with solvent G. After injecting a sample, proportion of solvent H was increased linearly to 12% in 3 min, to 40% in 14 min, and then to 100% in 5 min. PA-sugar chains were detected at an excitation wavelength of 310 nm and emission wavelength of 380 nm (Hase, 1994).

Quantification of PA-sugar chains

Digital chart recorder, Power Chrom™ (AD Instruments, NSW, Australia) or MacIntegrator™ (Rainin Instruments, MA, USA) system running on Macintosh™ computers (Apple Computer, CA, USA) were used for analysis of area and elution times of each peak. The amount of N-linked sugar chains contained in each tissue was quantified by adding the peak areas from all the fractions (M3-M11). The amount of each sugar chain was expressed as the molar percentage of the total N-linked sugar chains.

Exoglycosidase digestion

The PA-labeled oligosaccharides (~ 50 pmol) were digested in a volume of 20 µl for 18 h at 37°C using following enzymes (Table 2): *Diplococcus pneumoniae* β-galactosidase (Roche Diagnostics, Basel, Switzerland), specific for β(1,4)Gal, 50 µU/µl in 50 mM sodium acetate pH 6.0; jack bean β-galactosidase (Seikagaku Corporation, Tokyo, Japan), specific for β(1,3/4)Gal, 5 mU/µl in 50 mM sodium citrate pH 3.5; α1,3/4-L-fucosidase (Takara, Japan), specific for α(1,3/4)Fuc, 100 nU/µl in 50 mM sodium acetate pH 6.0; bovine kidney α-fucosidase (Glyko, Upper Heyford, UK), specific for α(1,6>1,2/3/4)Fuc, 1 mU/µl in 100 mM sodium citrate/phosphate pH 6.0; jack bean α-mannosidase (Seikagaku Corporation, Tokyo, Japan), specific for α(1,2/3/6)Man, 12.5mU/µl in 100 mM sodium acetate pH 4.5 containing 1 mM $ZnCl_2$.

The reaction was terminated by heating at 100°C for 5 min. The reaction mixture was centrifuged at 15,000 rpm for 20 min, and the supernatant was applied to HPLC.

Matrix-assisted laser-desorption ionization time-of-flight mass spectrometer (MALDI/TOF-MAS)

The molecular mass of PA-sugar chains and their isobaric monosaccharide compositions were determined by MALDI/TOF-MAS.

The PA-sugar chains were dissolved in water (1 pmol/μl). One μl of the sample was then mixed with 1 μl of the matrix solution (10 mg/ml 2,5-dihydroxybenzoic acid in 30% acetonitrile) and aliquots of 1 μl were deposited on a stainless steel target and analyzed after drying rapidly by an air drier. MALDI/TOF mass spectra of the samples were acquired using a REFLEX^{TM} Ⅲ spectrometer (Bruker-Franzen, Bremen, Germany) in the positive and reflector mode at an acceleration voltage of 20 kV and delayed ion extraction. Standard PA-sugar chains were used to achieve a two-point external calibration for mass assignment of ions. The mass spectra shown are the sum of at least 50 laser shots.

Quantitative real-time RT-PCR analyses of glycosyltransferase mRNAs

Total RNA from tissues was extracted by using a Quick Prep total RNA Extraction kit^{TM} (Amersham Biosciences) and 1 μg of total RNA was reverse-transcribed with Oligo (dT) primer (Promega) in a volume of 20 μl by SUPERSCRIPT^{TM} II (Life Technologies, Inc.) as follows. The following components were added to a nuclease-free microcentrifuge tube: 1 μl of Oligo $(dT)_{12\text{-}18}$ (500 μg/ml), 1 μl of total RNA (1 μg/μl) and 7 μl of distilled water. The mixture was heated to 70 °C for 10 min, and quickly chilled on ice. The contents of the tube were briefly centrifuged and the following components were added: 2 μl of 10X PCR Buffer (Life Technologies, Inc.), 2 μl of 0.1 M DTT (Life Technologies, Inc.) and 4 μl of 2.5 mM dNTP Mix (Promega) and 2 μl of 25 mM $MgCl_2$ (Promega). The contents of the tube were mixed gently and incubated at 42 °C for 5 min. After 1 μl (200 units) of

SUPERSCRIPT™ II addition the tube was mixed by pipetting gently up and down, and then incubated for 50 min at 42 °C. The reaction was terminated by heating at 70 °C for 15 min. The reaction mixture was diluted with distilled water at 1:100 and used for RT-PCR analysis.

RT-PCR was carried out using a LightCycler™ System (Roche), which allows amplification and detection (by fluorescence) of the amplified products in the same tube, using a kinetic approach. LightCycler PCR reactions were set up in microcapillary tubes using 2 μl of cDNA and 18 μl of a SYBR Green I master mix containing upstream and downstream PCR primers (0.5 μM), $MgCl_2$ (3 mM, Roche) and DNA master SYBR Green I (LightCycler-FastStart DNA Master SYBR Green I kit™, Roche). The following oligonucleotide primers specific for mouse Fuc-T Ⅷ (GenBank accession no. NM016893), Fuc-T Ⅸ (accession no. NM010243), β1-4Gal-T Ⅰ (accession no. E02227), Gn-T Ⅲ (accession no. NM010795) and GAPDH (accession no. M32599) were used.

Fuc-T Ⅷ:	CCAAGCAGAAGACGCAGACTA (sense)
	TAAAGAGGCGTTCCACCAGT (antisense)
Fuc-T Ⅸ:	CCTCCCTTGAGGACCATGTA (sense)
	TTTCCAGTGCTCGTTATCACA (antisense)
β1-4Gal-T Ⅰ:	TGTCAACATGCTGTGCCTTT (sense)
	GTGGCACATTTCCTTTGCTT (antisense)
Gn-T Ⅲ:	GGAGGGGATAAGGTGGTGTT (sense)
	CCTGTAATGGGCAACAGTCC (antisense)
GAPDH:	CTGAGCATCTCCCTCACAAT (sense)
	ATTCAAGAGAGTAGGGAGGG (antisense).

Length of amplified products using each primer pairs ranged from 100 to 150 bp. After initial denaturation at 95 °C for 10 min, reactions were repeated 45 times using

following parameters: 95 °C for 15 s, primer annealing at 60 °C for 5 s and primer extension at 72 °C for 5 s. Following each cycle, the fluorescent readings of the double-stranded products were done. At the end of each run, melting curve profiles were produced to confirm amplification of specific transcripts.

Cycle-to-cycle fluorescence emission readings were analyzed using LightCycler Software™ Ver. 3.3 (Roche). The transcriptional levels in E12 of each glycosyltransferase gene were used as control (= 100). The relative transcriptional levels in each developmental stage were corrected by normalization with the GAPDH mRNA level.

Results

Structural analysis of the major N-linked sugar chains expressed in adult mouse brain

I first determined the structures of the major N-linked sugar chains expressed in the CNS of adult mouse brain. More than 40 peaks after reverse-phase HPLC were collected from the PA-sugar chains prepared from adult ICR mouse brain. Each peak collected was re-applied to size-fractionation HPLC to measure precise mannose unit value (MU). I thus obtained two-dimensional map of 25 pyridylaminated N-linked sugar chains expressed in adult mouse brain with two indices consisting of mannose unit (MU) measured by size-fractionation HPLC and glucose unit (GU) measured by reverse-phase HPLC (Fig. 3). Since peaks 16 and 17 were mapped to the same position on the two-dimensional map (GU = 14.1, MU = 6.1), I separated these two sugar chains by another reverse-phase HPLC using CLC-ODS column as reported (Tomiya et al. 1988). I determined the structures of 19 PA-sugar chains from adult mouse brain by comparing their positions on the two-dimensional map against those of standard PA-sugar chains as previously described (Otake et al., 2001). The other six PA-sugar chains did not coincide with any standard PA-sugar chains, thus I identified their structures by exoglycosidase digestion and MALDI/TOF-MAS as following. The substrate specificity of the exoglycosidases used in this study is summarized in Table 2.

The PA-Sugar chain peak 8 (GU = 8.5, MU = 6.8) was sequentially digested with α1,3/4-L-fucosidase and *Diplococcus pneumoniae* β-galactosidase. One Fuc and Gal residue were released after each step, respectively, and changed their positions on the two-dimensional map (GU = 10.4, MU = 6.2; GU = 10.9, MU = 5.5) (Fig. 4a). No Gal residues were released when the sugar chain was further digested with jack bean β-galactosidase. After α1,3/4-L-fucosidase and *Diplococcus pneumoniae*

β-galactosidase digestion, the product was digested with bovine kidney α-fucosidase. One Fuc residue was released (GU = 8, MU = 5.3), which suggested the presence of core fucose residue. The final digested product coeluted on the reverse-phase HPLC with the sugar chain that was prepared from the standard PA-sugar chain H5.1 (see Table 1) by partial digestion with jack bean α-mannosidase to release one Man residue. Therefore, peak 8 was suggested to contain hybrid type sugar chain with four Man residues with bisecting GlcNAc. Further analysis was performed by MALDI/TOF-MAS which showed the monoisotopic mass of the MH^+ ion of this PA-sugar chain to be 2011.97, indicating the isobaric monosaccharide composition of H5N4F2 (Fig. 5a and see "*Abbreviations*"). All together, this peak 8 sugar chain structure was determined to be LewisX-H4FB as shown in Table 1.

The PA-sugar chains, peak 18 (GU 10.8, MU 6.7) and 19 (GU 11.3, MU 6.9), were digested with α1,3/4-L-fucosidase (Fig. 4b). In both cases, one Fuc residue was released, and their products were mapped to the same position on the two-dimensional map (GU 14.1, MU 6.1). However the structure of the two products were different from each other as discussed below. Further digestion was performed with *Diplococcus pneumoniae* β-galactosidase resulting in a release of one Gal residue in both cases. These digested products were mapped to the same position (GU 13.4, MU 5.2). The final digested products coeluted on the reverse-phase HPLC with the standard PA-sugar chain BA-2 (see Table 1), suggesting that these two sugar chains contained BA-2 structure with one LewisX epitope on the non-reducing ends of either the α1-6 or 1-3 Man branch. The original two PA-sugar chains, peak 18 and 19, were digested with α1,3/4-L-fucosidase. The digested products could be separated by the reverse-phase HPLC of CLC-ODS column, and then they coeluted with the standard PA-sugar chain Ga-BA-2 and Gb-BA-2 (see Table 1), respectively. These results indicate the sugar chains, peak 18 and 19 were LewisXa-BA-2 and LewisXb-BA-2

respectively (see Table 1).

The PA-sugar chain peak 22 (GU 9.3, MU 6.6) was digested with α1,3/4-L-fucosidase and *Diplococcus pneumoniae* β-galactosidase, but no Fuc and Gal residues were released (Fig. 4c). When the sugar chain was digested with jack bean β-galactosidase, two Gal residues were released (GU 9.0, MU 5.3). This result suggested all the Gal residues in this structure were connected via β1-3 linkages. The digested product coeluted on the reverse-phase HPLC with the standard PA-sugar chain A2G0F (see Table 1). Therefore, the peak 22 sugar chain was determined to be A2G'2F (see Table 1).

The PA-sugar chain peak 23 (GU 8.4, MU 7.6) was not susceptible to digestion with *Diplococcus pneumoniae* β-galactosidase (Fig. 4d). When sequentially digested with jack bean β-galactosidase and α1,3/4-L-fucosidase, one Gal residue was released (GU 8.3, MU 6.6), suggesting the Gal residue were connected via β1-3 linkage on the non-reducing end of the sugar chain, followed by the release of one Fuc residue (GU 9.6, MU 6.0). The product of this digestion coeluted with the standard PA-sugar chain A2G1(6)F (see Table 1) on the reverse-phase HPLC, but not with A2G1(3)F (GU 9.8) (see Table 1). After this fucosidase digestion, the product became susceptible to digestion with *Diplococcus pneumoniae* β-galactosidase and one Gal residue was released (GU 9.0, MU 5.3). The product of this digestion coeluted with the standard PA-sugar chain A2G0F (see Table 1). Accordingly, the results suggested that the sugar chain structure contained A2G0F structure with one LewisX epitope and one β1-3Gal residue on the non-reducing ends of α1-6 and α1-3 Man branch, respectively. Thus the peak 23 sugar chain was determined to be A2G1Fo(6)G'1(3)F (see Table 1). This sugar chain has not been reported in the brain before. Further analysis was performed to confirm this PA-sugar chain structure by using MALDI/TOF-MAS as shown in Fig. 5b. The monoisotopic mass

of the MH^+ ion of this PA-sugar chain was 2011.92, indicating the isobaric monosaccharide composition of H5N4F2 (see "*Abbreviations*"), which exactly matched with that of A2G1Fo(6)G'1(3)F (see Table 1).

The PA-sugar chain peak 25 (GU 9.3, MU 8.7) was susceptible to sequential digestion with α1,3/4-L-fucosidase followed by *Diplococcus pneumoniae* β-galactosidase. Two residues were released after each digestion (GU 14.7, MU 7.0; GU 13.4, MU 5.2) (Fig. 4e). The digested PA-sugar chains coeluted with the standard PA-sugar chain BA-2 (see Table 1) on the reverse-phase HPLC. Therefore, it was suggested that the sugar chain structure contained BA-2 structure with two LewisX epitopes on the non-reducing ends. Thus, its structure was determined to be LewisX2-BA-2 (see Table 1).

The brain-type N-linked sugar chains in adult mouse brain

The major N-linked sugar chains expressed in adult mouse whole brain and their amounts are shown in Table 3. I have identified about 70 % of total N-linked sugar chains expressed in adult mouse brain. N-linked sugar chains of oligomannose series (M5A, M6B, M7A, M7B, M8A, M9A) constituted 41.1 % of the total N-linked sugar chains in adult mouse brain, among which M5A was the most abundant. In this study, the brain-type structural features of N-linked sugar chains expressed in mouse brain were observed as follows.

(1) The sugar chains containing β1-4Gal residues on the non-reducing ends were expressed at a relatively low level and accounted for 12.8 % of the total N-linked sugar chains. About half of them contained outer-arm α1-3Fuc residues on the non-reducing ends, forming the LewisX epitopes (6.6 %). On the other hand, the sugar chains with GlcNAc residues on the non-reducing ends were expressed at a high level and accounted for 11.3 %.

These incompletely processed sugar chains were commonly observed among the biantennary sugar chains.

(2) N-linked sugar chains in the brain often carried bisecting GlcNAc, core Fuc or outer-arm Fuc accounting for 18.3, 21.7 and 6.6 % of the total amount of the N-kinked sugar chains, respectively.

(3) An interesting structural feature with no GlcNAc residue on the α1-3 Man branch was abundantly observed.

(4) Sugar chains containing Gal residues connected not only via β1-4 linkages but also via β1-3 linkages were observed and accounted for 1.4 %.

To study the variation in their expression pattern among individuals, the amounts of major N-linked sugar chains expressed in the cerebral cortices of five 21W mice were measured and are listed in Table 4. The amounts of N-linked sugar chains exceeding 1 % of the total amounts did not vary significantly among the samples, and their standard deviation (SD) was extremely small. This indicates that the expression of N-linked sugar chains is strictly regulated in mouse cerebral cortex so that there are little differences among individuals.

The developmental changes of N-linked sugar chain expression pattern in mouse cerebral cortex

To investigate the developmental changes of these brain-type sugar chain expression pattern, we analyzed the structures of the major N-linked sugar chains expressed in mouse cerebral cortex during development. Because of the result we obtained above, cerebral cortices of 2-30 mice were pooled, homogenized together and analyzed the sugar chain levels in only one preparation per point.

Representative HPLC elution profiles of N-linked sugar chains expressed in mouse cerebral cortex during development are shown in Fig. 6. The major N-linked sugar

chains expressed in mouse cerebral cortex during development and their amounts were shown in Table 5. In an oligomannose series, the expression level of M5A was lower than those of M9A, M8A and M6B in E12. But thereafter, the levels of M9A, M8A and M6B gradually reduced in the cerebral cortex during development. On the other hand, M5A showed a remarkable increase, reaching several times higher than those of other oligomannose type sugar chains by 12W. The developmental changes of the brain-type N-linked sugar chains can be summarized as follows.

(1) The amount of N-linked sugar chains containing β1-4Gal residues on the non-reducing ends was most abundant in E12 and reduced slightly in E16 (Fig. 7). On the other hands, the amount of N-linked sugar chains containing GlcNAc residues on the non-reducing ends were present at lower level in E12 and gradually increased during development (Fig. 7).

(2) The amount of N-linked sugar chains containing LewisX epitopes on the non-reducing ends was present at lower level in E12 and gradually increased during development, reaching their maximum on P7 and reduced slightly by 12W (Fig. 7).

(3) The amount of the N-linked sugar chains containing core Fuc and bisecting GlcNAc residues remained constant in the embryonic stage at relatively high level, increased further after birth, reaching the maximum on P7 and reduced slightly by 12W (Fig. 7).

(4) The amount of the N-linked sugar chains containing Gal residues connected via β1-3 linkages appeared after birth.

(5) The structural feature of N-glycosylation in the brain containing no GlcNAc residue on the α1-3 Man branch became abundant after P7.

These results show that most of the N-linked sugar chains were completely processed and the brain-type structural features were not prominent in the early

embryonic stage (E12) of the cerebral cortex. The expression levels of these brain-type sugar chains in the cerebral cortex increased during development.

"Brain type" sugar chain BA-2 and LewisX-BA-2 show similar expression profiles during development in mouse cerebral cortex

Among the brain-type sugar chains LewisX-BA-2 is particularly interesting, because its physiological significance during development has been clarified. LewisX-BA-2 is comprised of BA-2 and LewisX epitopes attached to BA-2 on the non-reducing ends (see Table 1). Its biosynthetic pathway is also mysterious since no enzymatic activities to transfer the Gal residues to the non-reducing ends of BA-2 have been detected (Nakakita et al. 1999). Therefore, I focused on the developmental changes of the BA-2 level and those of its related sugar chains, BA-1, Gal-BA-2 (BA-2 containing one or two Gal residues on the non-renducing ends) and LewisX-BA-2 (Fig. 8). The amount of BA-2 was low in E12, reached its maximum on P7, and reduced slightly by 12W. Interestingly, the expression profile of LewisX-BA-2 during development was very similar to that of BA-2 (Fig. 8). Gal-BA-2 was most abundant in E12, remarkably reduced on E16 and thereafter gradually reduced until 12W. The amount of BA-1 was low until P7 and remarkably increased by 12W.

Because I analyzed the backbone structures of all the N-linked sugar chains after neuraminidase treatments, I checked the possibility of LewisX-BA-2 being sialylated in the cerebral cortex in each developmental stage. Fig. 9 shows the comparisons of the HPLC patterns of N-linked sugar chains after neuraminidase treatments with the flow through fraction of the same sample after MonoQ-HPLC, which means unsialylated fraction, in mouse cerebral cortex of E12 and 12W. By normalizing the amounts against those of oligomannnose series, it has been shown that most of

LewisX-BA-2 was not sialylated during development (E12, E16, P0 and P7) or in the adult (12W) (E12; Fig. 9a, 12W; Fig. 9b and data not shown). It was also confirmed that LewisX-BA-2 was hardly detected in the sialylated fractions of the MonoQ-HPLC after neuraminidase digestion in the mouse cerebral cortex during development (data not shown).

The developmental changes of glycosyltransferase gene expressions in mouse cerebral cortex.

The expression levels of the following four glycosyltransferases that may be involved in production of brain-type sugar chains were analyzed.

(1) Fuc-T Ⅷ catalyzes the attachment of a Fuc residue to GlcNAc residue on the reducing end through α1-6 linkages forming a core fucose.

(2) Fuc-T Ⅸ catalyzes the attachment of a Fuc residue to GlcNAc residue of the type 2 chain, Galβ1-4GlcNAc-R, through α1-3 linkages. Among the α1-3Fuc-Ts family, LewisX epitope is formed mainly by Fuc-TⅨ in the brain (Kudo et al., 1998).

(3) Beta1-4Gal-T Ⅰ catalyzes the transfer of Gal to terminal GlcNAc residues on elongating sugar chains through β1-4 linkages. Though at least six β1-4Gal-Ts would be involved in the biosynthesis of N-linked sugar chains (Guo et al. 2001), β1-4Gal-T Ⅰ is expressed in most organs except for the brain (Lo et al. 1998).

(4) Gn-T Ⅲ catalyzes the attachment of a GlcNAc residue to a Man residue in the core region of N-linked sugar chains through β1-4 linkage forming a bisecting GlcNAc.

The results of real-time RT-PCR analysis on the mRNA levels of glycosyltransferase are shown in Fig. 10. The developmental changes in the levels

of Fuc-T Ⅷ, Fuc-TⅨ and Gn-T Ⅲ mRNA were similar in the cerebral cortex. They were detected at a lower level in E12, reached their maximum on P0, and reduced slightly by 12W. Sudden down regulation of β1-4Gal-T-Ⅰ gene expression happened between E12 to E16, relatively constant on P7 and slightly reduced by 12W.

Discussion

Characterization of the major N-linked sugar chains expressed in adult mouse brain

Numerous N-linked sugar chains including those characteristics for the brain are expressed in the brain (Shimizu et al. 1993; Chen et al., 1998; Zamze et al., 1998). In the present study I first analyzed the major N-linked sugar chains expressed in adult mouse brain by the previously developed method (Fujimoto et al. 1999; Otake et al. 2001) and determined their structures (Table 3 and see Table 1). Among the structures of six N-linked sugar chains I determined, one sugar chain structure (#23 in Table 1: A2G1Fo(6)G'1(3)F) was novel, which was identified for the first time in the brain. The amount of sugar chain I determined in the present study would consists of more than 70 % of total amount of N-linked sugar chains expressed in adult mouse brain. Thus, it became possible to determine the brain-type features of N-linked sugar chains expressed in mouse brain as described in the "*Results*".

Highly characteristic structural features observed in N-linked sugar chains in the brain were incompletely processed agalacto structure. Such sugar chains are considered to reflect the low expression levels of β1-4Gal-T genes in the brain compared with other organs (Lo et al. 1998). N-linked sugar chains in the brain often carry bisecting GlcNAc, core Fuc or outer-arm Fuc. The mRNA levels of Gn-T Ⅲ and Fuc-T Ⅷ were reported to be high in the brain (Miyoshi et al. 1997). The outer-arm Fuc residue is transferred mainly by Fuc-T-Ⅸ which was reported to be expressed at a high level in the brain (Kudo et al., 1998). Another interesting N-linked sugar chain expressed in the brain is BA-1, the sugar chain containing no GlcNAc residue on the α1-3 Man branch. N-linked sugar chains including such structural feature are observed abundantly in the brain (Chen et al. 1998). In the brain, β-hexosaminidase B removes the GlcNAc residue linked to the Manα1-3 branch

of BA-2 and converts BA-2 to BA-1 (Okamoto et al., 1999). The N-linked sugar chains containing Gal residues connected not only via β1-4 linkages but also via β1-3 linkages were observed. Recently the genes for mouse β1-3Gal-T have been cloned and shown to be expressed mainly in the brain (Hennet et al. 1998).

Changes in high mannose type sugar chain levels in the cerebral cortex during development

The amounts of M9A, M8A and M6B were higher than that of M5A at E12, however, their amounts gradually decreased in the cerebral cortex during development. On the other hand, the M5A content gradually increased during development, reaching several times higher than those of other oligomannose type sugar chains by 12W (Table. 5). Since the oligomannose N-linked sugar chains are present on the surface of neural cells (Schmitz et al. 1993), it has been reported that the oligomannose N-linked sugar chains would play important roles such as synaptic formation (Dontenwill et al. 1985) and myelination (Kuchler et al. 1989) in the CNS during development. Therefore, it is considered that the cell-surface oligomannose N-linked sugar chains would be particularly important and their expression should be strictly regulated in the cerebral cortex during development. Our result suggests that M5A has its own function in the brain that cannot be replaced by other high mannose sugar chains.

Formation of brain-type N-glycosylation pattern in the cerebral cortex during development

The N-linked sugar chains containing β1-4Gal residues on their non-reducing ends were abundant in E12. However, their amount drops suddenly following down regulation of β1-4Gal-T-Ⅰ expression between E12 to E16 in the brain (Fig. 10)

(Nakamura et al. 2001), resulting in an increase of sugar chains bearing GlcNAc residues on their non-reducing ends. This event is considered to be the first step in forming the brain-type N-glycosylation pattern. Rapid down regulation of the galactosylation level in the cerebral cortex happened in the stage of neuronal cell migration to their laminar position after their final mitotic division during development (Fig. 11). The neurogenesis commences around embryonic day 11 (E11) and continues until about E16 or E17, followed by the generation of astrocytes and then oligodendrocytes during development (Jacobson, M. 1991). Therefore, it is possible that the down regulation of β1-4Gal-T-Ⅰ gene expression occurs in neuronal and glial cells which completed their final mitotic division, and the sugar chains containing GlcNAc residues on the non-reducing ends would play important roles for regulating their differentiation or proliferation.

The levels of the N-linked sugar chains containing LewisX epitope on the non-reducing ends were relatively low in E12, reaching the maximum on P7 and reduced slightly by 12W during development. I observed that such sugar chains often carried a bisecting GlcNAc and/or a core Fuc residue in the cerebral cortex during development. Sugar chains containing these structural elements showed a similar developmental profile in their expression levels. Furthermore, the gene expression of the key enzymes involved in their biosyntheses showed developmental changes consistent with the changes in the levels of sugar chains (Fig. 10). Therefore, these structural elements would be regulated and play functional roles cooperatively in the cerebral cortex during development as will be discussed below.

The expression of the N-linked sugar chains containing Gal residues connected via β1-3 linkages appeared after birth. The expression of the sugar chains containing no GlcNAc residue on the α1-3 Man branch, such as BA-1, appeared after P7. Such structural elements make the expression pattern of N-linked sugar chains in the brain

more complex and more characteristic. But the physiological significances are totally unknown. Since these N-linked sugar chains appeared in the postnatal developmental stage, it is possible that they are expressed only in some populations of glial cells, not in neurons.

The cerebral cortex is formed via complex, but highly ordered processes containing migration, differentiation and maturation of neural cells. Changes in a great variety of characteristic sugar chains would be explained mostly by the regulation of gene expression of several glycosyltrasferases and glycosidases. In the present study, four representative enzymes among them showed development-dependent changes in their mRNA levels (Fig. 10), and the changes in their expression levels corresponded to the sugar chain expression patterns.

There are yet little evidences indicating that the N-linked sugar chains carrying brain-type structural elements play important roles in the CNS during development. It is possible that the brain-type structural elements would function in the CNS during development by binding to specific receptors such as lectin. The brain-type N-glycosylation pattern are formed relatively late during development, thus it is speculated that they would play important roles in maintaining normal brain functions after development rather than during development.

Regulation of biosynthesis of BA-2 and its related sugar chains in the CNS during development

Although the functions of most of the N-linked sugar chains are unclear at present, there are rare cases in which the significance of sugar chains in the brain during development has been proposed such as LewisX-BA-2. It was reported that the immunoreactivity of the rat monoclonal antibody L5 is associated with a complex-type N-linked sugar chain of glycoproteins, LewisX-BA-2 (Streit et al. 1996).

LewisX-BA-2 has typical structural features of N-linked sugar chains expressed in the brain such as bisecting GlcNAc, core Fuc and LewisX epitopes. The L5 epitope has been implicated in the outgrowth of astrocyte processes on extracellular matrix component during postnatal development of mouse cerebellum (Streit et al. 1993; Streit and Stern 1995). In the present study, I observed that the level of LewisX-BA-2 was low in E12, reaching the maximum at P7 in mouse cerebral cortex (Fig. 8). The increase in LewisX-BA-2 level in the cerebral cortex corresponded to the stage when most astrocytes have already been produced. It is possible that LewisX-BA-2 would predominantly be expressed in astrocyte processes and be associated with their extension during development.

BA-2 and BA-1 were previously reported to be expressed abundantly and specifically in mouse brain and their levels change characteristically during development (Shimizu et al. 1993; Nakakita et al., 1998). Their physiological roles in the CNS development are totally unknown. The expression of LewisX-BA-2 changed similarly to that of BA-2 during development (Fig. 8). Therefore, it is possible that LewisX-BA-2 would be formed after the production of BA-2, suggesting that the expression of LewisX-BA-2 would be regulated according to the BA-2 level. However, no β1-4Gal-T activity to galactosylate BA-2 was detected in the brain of P10 mouse in comparison to E13 brain in which some degree of the activity was detected (Nakakita et al., 1999). Thus the biosynthetic pathway of LewisX-BA-2 in adult mouse brain remains to be elucidated. It is possible that the β1-4Gal-T expressed in the brain would recognize not only the BA-2 structure but also the structure of glycoprotein on which it is expressed.

Conclusion

In the present study, I characterized the N-linked sugar chains expressed in mouse

cerebral cortex during development comprehensively. The present results will form important basis for elucidating the regulatory mechanism and physiological significance of N-linked sugar chains in the CNS during development.

Acknowledgements

I wish to express my gratitude to many people in completing my thesis and research during this three years.

Prof. K. Ikenaka, my supervisor and head of Laboratory of Neural Information at National Institute of Physiological Sciences, Okazaki National Research Institutes, I would like to thank specially for introducing me so exciting theme as glycobiology and for his valuable guidance throughout this study.

Dr. I. Fujimoto, I would like to thank for reading the draft and making a number of helpful suggestions.

Prof. S. Hase and S. Nakakita, Department of Chemistry, Graduate School of Science, Osaka University, I wish to thank for various help and valuable advice.

I thank my colleagues for useful discussions, especially for Mr. A. Ishii, Dr. K. Sakuma and Dr. A. Deguchi.

Finally, I thank Ms. I. Ito for her technical assistance of HPLC analysis, Ms. Y. Makino and Mr. T. Nakamura for their technical assistance of MALDI/TOF-MAS analysis.

References

Albach, C., Klein, R.A., and Schmitz, B. (2001) Do rodent and human brains have different N-glycosylation patterns. *Biol. Chem.*, **382**, 187-194.

Allendoerfer, K.L., and Shatz, C.J. (1994) The subplate, a transient neocortical structure: its role in the development of connections between thalamus and cortex. *Annu. Rev. Neurosci.*, **17**, 185-218.

Bayer, S.A., and Altman, J. (1991) *Neocortical Development.* Raven Press, New York.

Chen, Y., Wing, D.R., Guile, G.R., Dwek, R.A., Harvey, D.J., and Zamze, S. (1998) Neutral N-glycans in adult rat brain: complete characterization reveals fucosylated hybrid and complex structure. *Eur. J. Biochem.*, **251**, 691-703.

Dontenwill, M., Roussel, G., and Zanetta, J.P. (1985) Immunohistochemical localization of a lectin-like molecule, R1, during the postnatal development of the rat cerebellum. *Brain Res.*, **349**, 245-52.

Fujimoto, I., Menon, K.K., Otake, Y., Tanaka, F., Wada, H., Takahashi, H., Tsuji, S., Natsuka, S., Nakakita, S., Hase, S., and Ikenaka, K (1999) Systematic analysis of N-linked sugar chains from whole tissue employing partial automation. *Anal. Biochem.*, **267**, 336-343.

Furukawa, K., Takamiya, K., Okada, M., Inoue, M., Fukumoto, S., and Furukawa, K. (2001) Novel functions of complex carbohydrates elucidated by the mutant mice of

glycosyltransferase genes. *Biochim. Biophys. Acta*, **1525**, 1-12.

Gooi, H.C., Feizi, T., Kapadia, A., Knowles, B.B., Solter, D., and Evans, M.J. (1981) Stage-specific embryonic antigen involves alpha 1 goes to 3 fucosylated type 2 blood group chains. *Nature*, **292**, 156-8.

Guo, S., Sato, T., Shirane, K., and Furukawa, K (2001) Galactosylation of N-linked oligosaccharides by human β-1,4-galactosyltransferase Ⅰ, Ⅱ, Ⅲ, Ⅳ, Ⅴ and Ⅵ expressed in Sf-9 cells. *Glycobiology*, **11**, 813-820.

Hakomori, S., Nudelman E., Levery, S., Solter, D., Knowles, B.B. (1981) The hapten structure of a developmentally regulated glycolipid antigen (SSEA-1) isolated from human erythrocytes and adenocarcinoma: a preliminary note. *Biochem. Biophys. Res. Commun.*, **100**, 1578-86.

Hase, S. (1994) High performance liquid chromatography of pyridylaminated saccharides. *Methods Enzymol*., **230**, 225-237.

Hase, S., Ikenaka, K., Mikoshiba, K., and Ikenaka, T. (1988) Analysis of tissue glycoprotein sugar chains by two-dimensional high-performance liquid chromatographic mapping. *J. Chromatogr.*, **434**, 51-60.

Hase, S., Ikenaka, T., and Matsushima, Y. (1981) A high sensitive method for analysis of sugar moieties of glycoproteins by fluorescence labeling. *J. Biochem.*, **90**, 407-14.

Hase, S., Natsuka, S., Oku, H., and Ikenaka, T. (1987) Identification method for

twelve oligomannose-type sugar chains thought to be processing intermediates of glycoproteins. *Anal. Biochem.*, **167**, 321-6.

Hennet, T., Dinter, A., Kuhnert, P., Mattu, T.S., Rudd, P.M., and Berger, E.G. (1998) Genomic cloning and expression of three murine UDP-galactose: β-N-acetylglucosamine β1,3-galactosyltransferase genes. *J. Biol. Chem.*, **273**, 58-65.

Helenius, A., and Aebi, M. (2001) Intracellular functions of N-linked glycans. *Science*, **291**, 2364-2369.

Ioffe, E., and Stanley, P. (1994) Mice lacking N-acetylglucosaminyltransferase I activity die at mid-gestation, revealing an essential role for complex or hybrid N-linked carbohydrate. *Proc. Natl. Acad. Sci.*, **91**, 728-732.

Jacobson, M. (1991) *Developmental Neurobiology.* Prenum Press, New York.

Kobata, A., and Ginsburg, V. (1969) Oligosaccharides of human milk. II. Isolation and characterization of a new pentasaccharides, lacto-N-fucopentaose 3. *J. Biol. Chem.*, **244**, 5496-502.

Kuchler, S., Rougon, G., Marschal, P., Lehmann, S., Reeber, A., Vincendon, G., and Zanetta, J.P. (1989) Location of a transiently expressed glycoprotein in developing cerebellum delineating its possible ontogegetic roles. *Neuroscience*, **33**, 111-24.

Kudo, T., Ikehara, Y., Togayachi, A., Kaneko, M., Hiraga, T., Sasaki, K., and Narimatsu, H. (1998) Expression cloning and characterization of a novel murine

α1,3-Fucosyltransferase, mFuc-T**IX**, that synthesizes the Lewis x (CD15) epitope in brain and kidney. *J. Biol. Chem.*, **273**, 26729-26738.

Kurachi, K., and Davie, E.W. (1982) Isolation and characterization of a cDNA coding for human factor Ⅸ. *Proc. Natl. Acad. Sci.*, **79**, 6461-6464.

Levison, S.W., and Goldman, J.E. (1993) Both oligodendrocytes and astrocytes develop from progenitors in the subventricular zone of postnatal rat forebrain. *Neuron*, **10**, 201-212.

Lo, N.W., Shaper, J.H., Pevsner, J., and Shaper, N.L. (1998) The expanding β4-galactosyltransferase gene family: messages from the databanks. *Glycobiology*, **8**, 517-526.

Luskin, M.B., Pearlman, A.L., and Sanes, J.R. (1988) Cell linage in the cerebral cortex of the mouse studied in vivo and in vitro with a recombinant retrovirus. *Neuron*, **1**, 635-647.

Luskin, M.B., and McDermott, K. (1994) Divergent lineages for oligodendrocytes and astrocytes originating in the neonatal forebrain subventricular zone. *Glia*, **11**, 211-226.

Makino, Y., Omichi, K., Kuraya, N., Ogawa, H., Nishimura, H., Iwanaga, S., and Hase, S. (2000) Structural analysis of N-linked sugar chains of human blood clotting factor Ⅸ. *J. Biochem.*, **128**, 175-180.

Metzler, M., Gertz, A., Sarkar, M., Schachter, H., Schrader, J.W., and Marth, D.J. (1994) Complex asparagine-linked oligosaccharides are required for morphogenic events during post-implantation development. *EMBO J.*, **13**, 2056-2065.

Miyoshi, E., Uozumi, N., Noda, K., Hayashi, N., Hori, M., and Taniguchi, N. (1997) Expression of α1-6 fucosyltransferase in rat tissues and human cancer cell lines. *Int. J. Cancer*, **72**, 1117-1121.

Nakakita, S., Natsuka, S., Ikenaka, K., and Hase, S. (1998) Development-dependent expression of complex-type sugar chains specific to mouse brain. *J. Biochem.*, **123**, 1164-1168.

Nakakita, S., Menon, K.K., Natsuka, S., Ikenaka, K., and Hase, S. (1999) β1-4 galactosyltransferase activity of mouse br
ain as revealed by analysis of brain-specific complex-type N-linked sugar chains. *J. Biochem.*, **126**, 1161-1169.

Nakamura, N., Yamakawa, N., Sato, T., Tojo, H., Tachi, C., and Furukawa, K. (2001) Differential gene expression of β-1,4-galactosyltransferase Ⅰ, Ⅱ and Ⅴ during mouse brain development. *J. Neurochem.*, **76**, 29-38.

Okamoto, Y., Omichi, K., Yamanaka, S., Ikenaka, K., and Hase, S. (1999) Conversion of brain-specific complex type sugar chains by N-acetyl-β-D-hexosaminidase B. *J. Biochem.*, **125**, 537-540.

Otake, Y., Fujimoto, I., Tanaka, F., Nakagawa, T., Ikeda, T., Menon, K.K., Hase, S.,

Wada, H., and Ikenaka, K. (2001) Isolation and characterization of an N-linked sugar oligosaccharide that is significantly increased in sera from patients with non-small cell lung cancer. *J. Biochem.*, **129**, 537-542.

Parekh, R.B., Tse, A.G.D., Dwek, R.A., Williams, A.F., and Rademacher, T.W. (1987) Tissue-specific N-glycosylation, site-specific oligosaccharide patterns and lentil lection recognition of rat Thy-1. *EMBO J.*, 6, 1233-1244.

Price, J., and Thurlow, L. (1988) Cell lineage in the rat cerebral cortex: a study using retroviral-mediated gene transfer. *Development*, **104**, 473-483.

Sauvageot, C.M., and Stiles, C.D. (2001) Molecular mechanisms controlling cortical gliogenesis. *Curr. Opin. Neurobiol.*, **12**, 244-249.

Schmitz, B., Peter-Katalinic, J., Egge, H., and Schachner, M. (1993) Monoclonal antibodies raised against membrane glycoproteins from mouse brain recognize N-linked oligomannosidic glycans. *Glycobiology*, **3**, 609-17.

Shimizu, H., Ochiai, K., Ikenaka, K., Mikoshiba, K., and Hase, S. (1993) Structures of N-linked sugar chains expressed mainly in mouse brain. *J. Biochem.*, **114**, 334-338.

Shimoda, Y., Tajima, Y., Osanai, T., Katsume, A., Kohara, M., Kudo, T., Narimatsu, H., Takashima, N., Ishii, Y., Nakamura, S., Osumi, N., and Sanai, Y. (2002) Pax6 controls the expression of Lewis x epitope in the embryonic forebrain by regulating alpha 1,3-fucosyltransferase IX expression. *J. Biol. Chem.*, **277**, 2033-2039.

Streit, A., Nolte, C., Rasony, T., and Schachner, M. (1993) Interaction of astrochondrin with extracellular matrix components and its involvement in astrocyte process formation and cerebellar granule cell migration. *J. Cell. Biol.*, **120**, 799-814.

Streit, A., and Stern, C.D. (1995) L5: A carbohydrate epitope involved in neural development. *Biol. Cell*, **84**, 63-67.

Streit, A., Yuen, C.T., Loveless, R.W., Lawson, A.M., Finne, J., Schmitz, B., Feizi, T., and Stern, C.D. (1996) The Le^X carbohydrate sequence is recognized by antibody to L5, a functional antigen in early neural development. *J. Neurochem.*, **66**, 834-844.

Sun, X.Z., Takahashi, S., Cui, C., Zhang, R., Sakata-Haga, H., Sawada, K., and Fukui, Y. (2002) Normal and abnormal neuronal migration in the developing cerebral cortex. *J. Med. Invest.*, **49**, 97-110.

Tomiya, N., Awaya, J., Kurono, M., Endo, S., Arata, Y., and Takahashi, N. (1988) Analysis of N-linked oligosaccharides using a two-dimensional mapping technique. *Anal. Biochem.*, **171**, 73-90.

Trenkner, E., and Sarkar, S. (1977) Microbial carbohydrate specific antibodies distinguished between different stages of differentiating mouse cerebellum. *J. Supramol. Struct.*, **6**, 465-472.

Voigt, T. (1989) Development of glial cells in the cerebral wall of ferrets: direct tracing of their transformation from radial glia into astrocytes. *J. Comp. Neurol.*, **289**, 74-88.

Woodruff, R.H., Tekki-Kessaris, N., Stiles, C.D., Rowitch, D.H., and Richardson, W.D. (2001) Oligodendrocyte development in the spinal cord and telencephalon: common themes and new perspective. *Int. J. Dev. Neurosci.*, **19**, 379-385.

Yoshimi, Y., Yamazaki, S., and Ikekita, M. (1999) Developmental changes in Asn-linked neutral oligosaccharides in murine cerebrum. *Biochim. Biophys. Acta*, **1426**, 69-79.

Zamze, S., Harvey, D.J., Chen, Y., Guile, G.R., Dwek, R.A., and Wing, D.R. (1998) Sialylated N-glycans in adult rat brain tissue: a widespread distribution of disialylated antennae in complex and hybrid structures. *Eur. J. Biochem.*, **258**, 243-270.

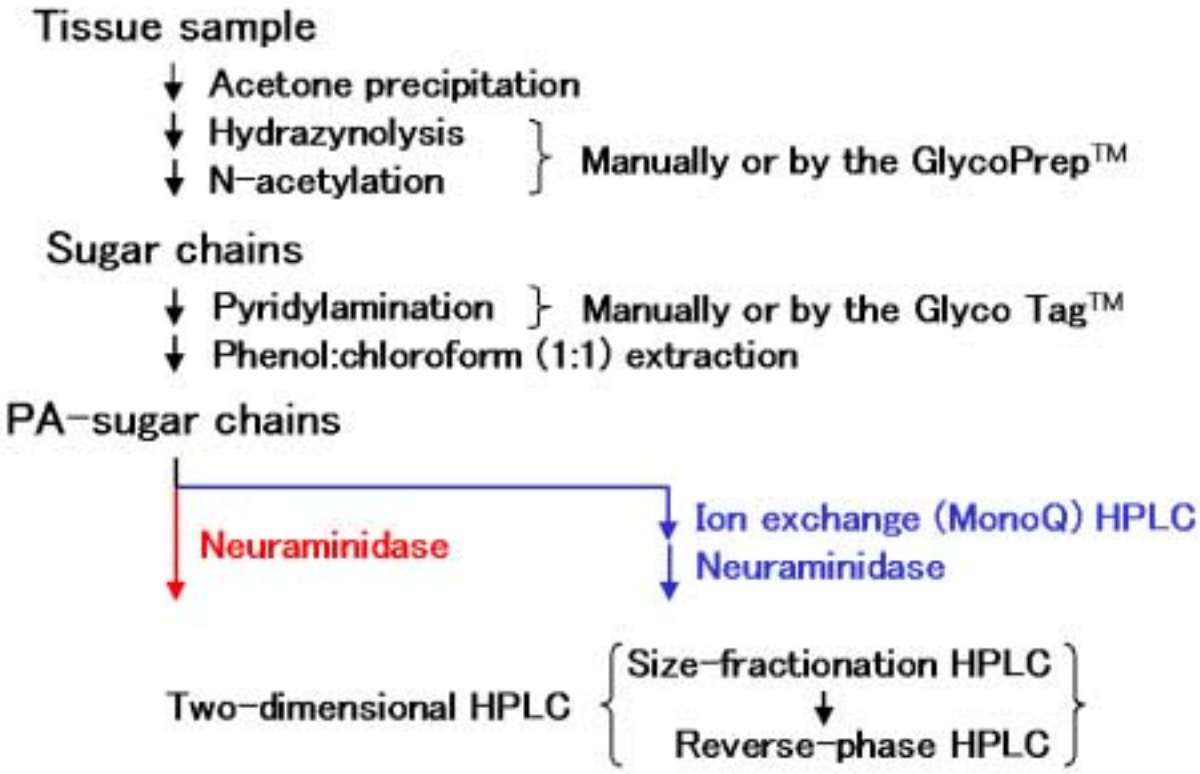

Fig. 1. *Outline of the general strategy employed in this study.* Tissue samples were homogenized with nine-fold volume of acetone, and the precipitates were lyophilized. Samples were hydrazinolized to release sugar chains and then N-acetylated. These steps were performed manually or by the automated GlycoPrep™. The amount of samples for hydrazinolysis was 1 to 2 mg. After lyophilization, sugar chains were converted to pyridylamino (PA) derivatives manually or by the automated GlycoTag™. Excess reagents were removed by phenol:chloroform (1:1) extraction. The sugar chain backbone of the PA-sugar chains containing sialylated and neutral components was totally detected by two-dimensional HPLC (Size-fractionation HPLC and reverse-phase HPLC, see Fig. 2) after neuraminidase digestion (red). The sialic acid component was also detected by ion exchange HPLC followed by neuraminidase digestion and two-dimensional HPLC (blue).

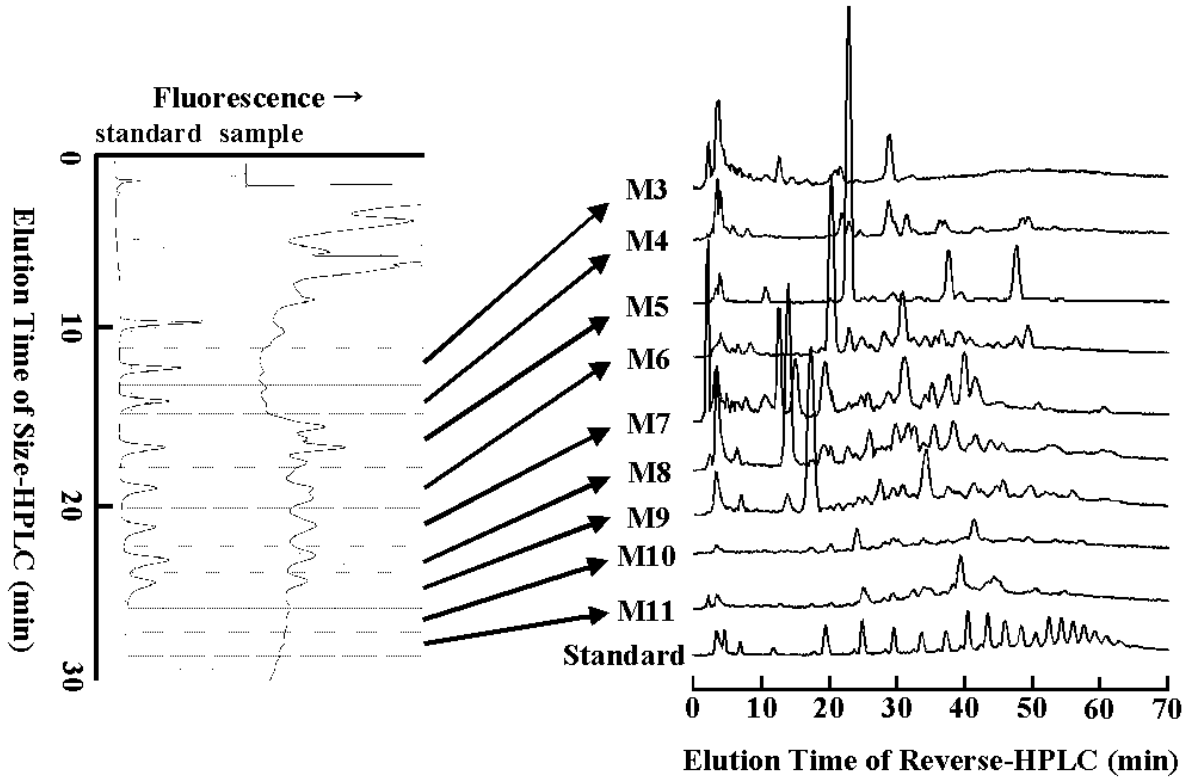

Fig. 2. *Two-dimensional HPLC analysis of PA-sugar chains.* PA-sugar chains were detected by the fluorescence detector and at femtomole levels, and excellent separation was achieved by a combination of size-fractionation HPLC and reverse-phase HPLC. Sugar chain backbones of neuraminidase-treated PA-sugar chains were analyzed by two-dimensional HPLC composed of size-fractionation HPLC and reverse-phase HPLC. Any impurities of non-sugar nature, if present in these fractions, were removed along with the flow thorough. Size fractionation was performed by collecting nine samples at the elution time of the mannose unit standards M3, M4B, M5A, M6B, M7A, M8A and M9A (see Table 1). The M10 and M11 were sequentially fractionated during 1.2 min from M9 fraction end time. These individual fractions were further characterized by a Cosmosil 5C18-P reverse-phase HPLC column. The PA-sugar chains were detected at an excitation

wavelength of 320 nm and an emission wavelength of 400 nm. Essentially al of the N-linked sugar chains elute after 10 min, while O-linked sugar chains partially recovered using our procedures and elute earlier together with impurities.

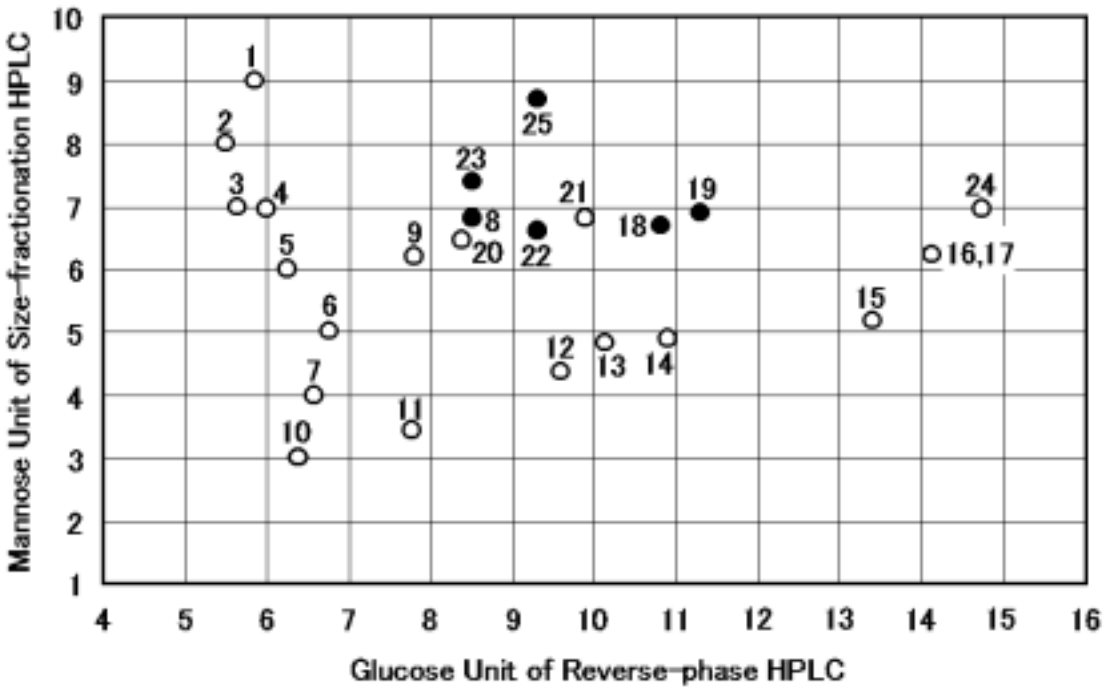

Fig. 3. *Two-dimensional HPLC map for PA-sugar chains from adult mouse brain.* The vertical axis indicates mannose unit values (MU) calculated from the elution time on size-fractionation HPLC, and the horizontal axis indicates glucose unit values (GU) from reverse-phase HPLC. The numbers of the plotted points indicates the PA-sugar chains shown in Table 1 and 3. The structures of 19 PA-sugar chains from adult mouse brain were determined by comparing their positions on the two-dimensional map against those of standard PA-sugar chains (open circle). The positions of the other 6 PA-sugar chains (closed circle) did not coincide on the two-dimensional map with those of any standard PA-sugar chains, their structures were determined by exoglycosidase digestion and MALDI/TOF-MAS.

(a)

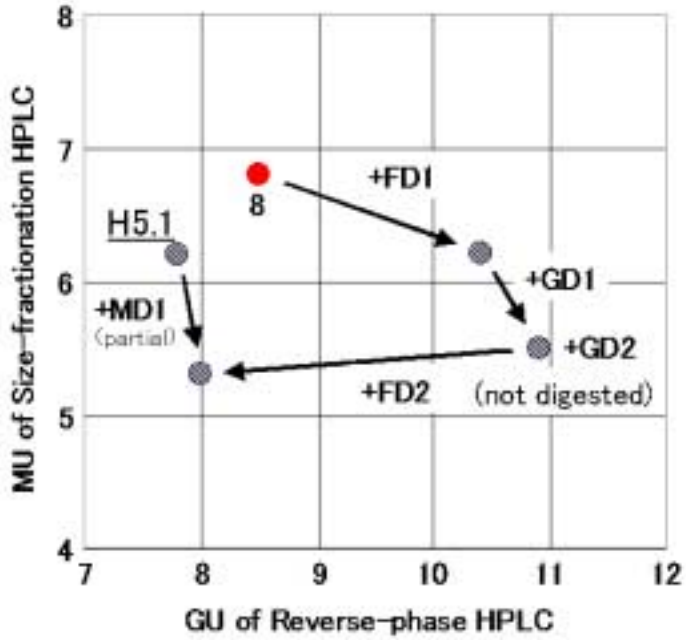
MU of Size-fractionation HPLC
GU of Reverse-phase HPLC
8
7
6
5
4
7
8
9
10
11
12
H5.1
8
+FD1
+GD1
+MD1
(partial)
+GD2
+FD2
(not digested)

(b)

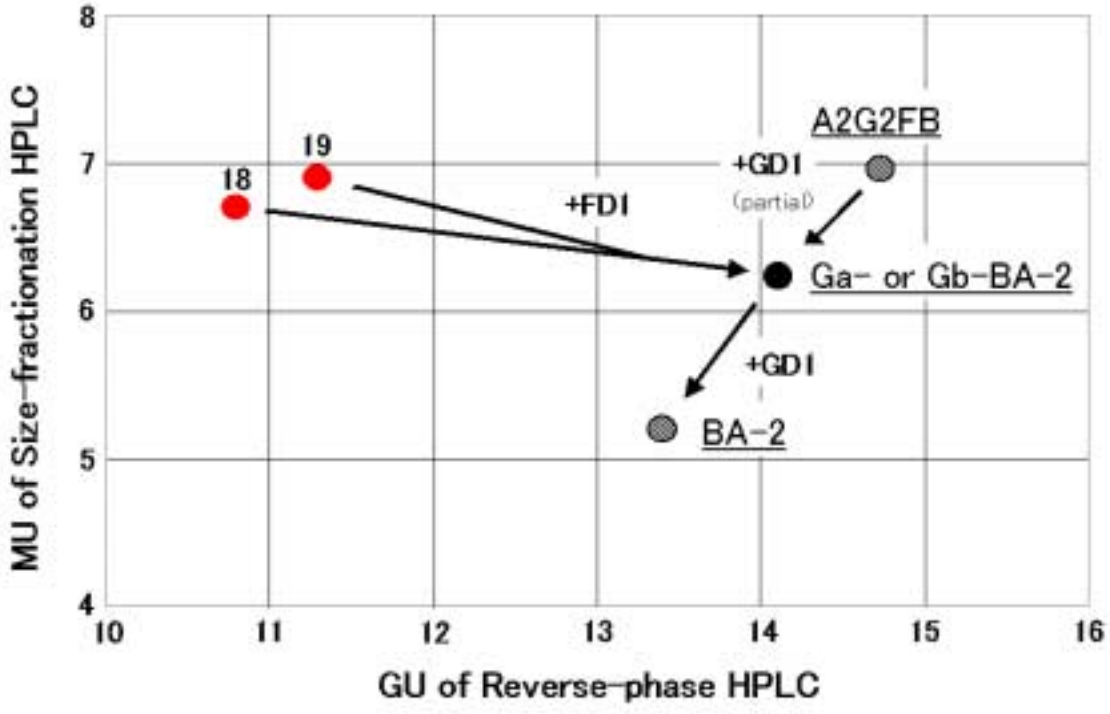
MU of Size-fractionation HPLC
GU of Reverse-phase HPLC
8
7
6
5
4
10
11
12
13
14
15
16
19
18
+FD1
A2G2FB
+GD1
(partial)
Ga- or Gb-BA-2
+GD1
BA-2

(c)

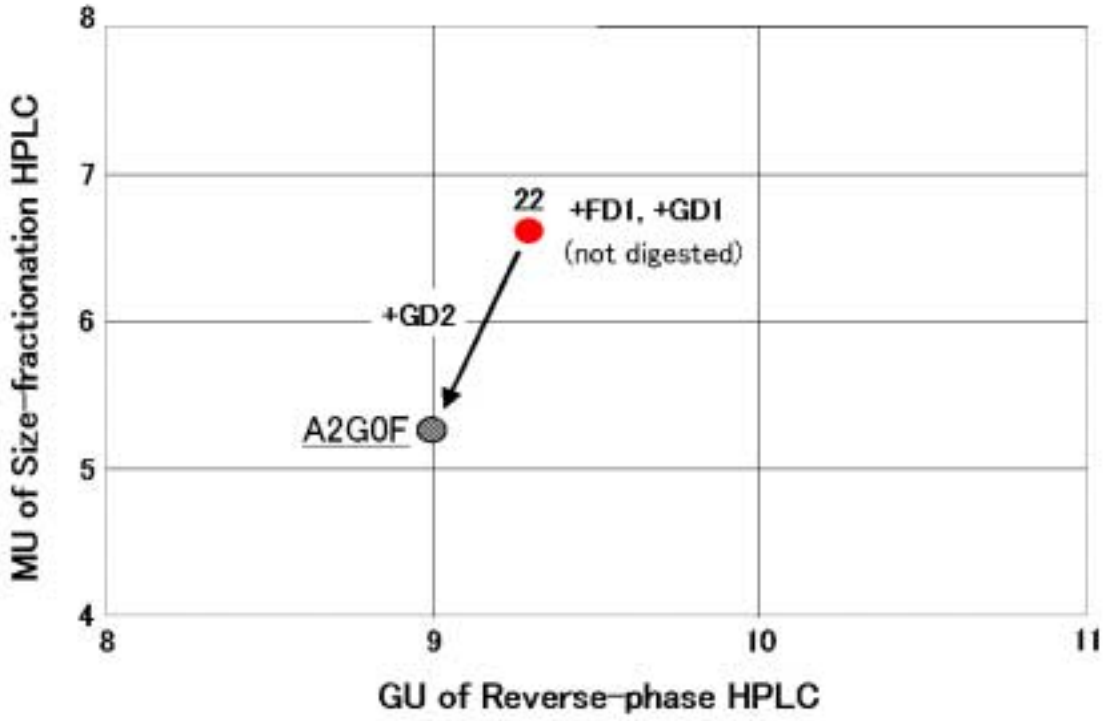
MU of Size-fractionation HPLC
GU of Reverse-phase HPLC
22
+FD1, +GD1
(not digested)
+GD2
A2G0F
8
7
6
5
4
8
9
10
11

(d)

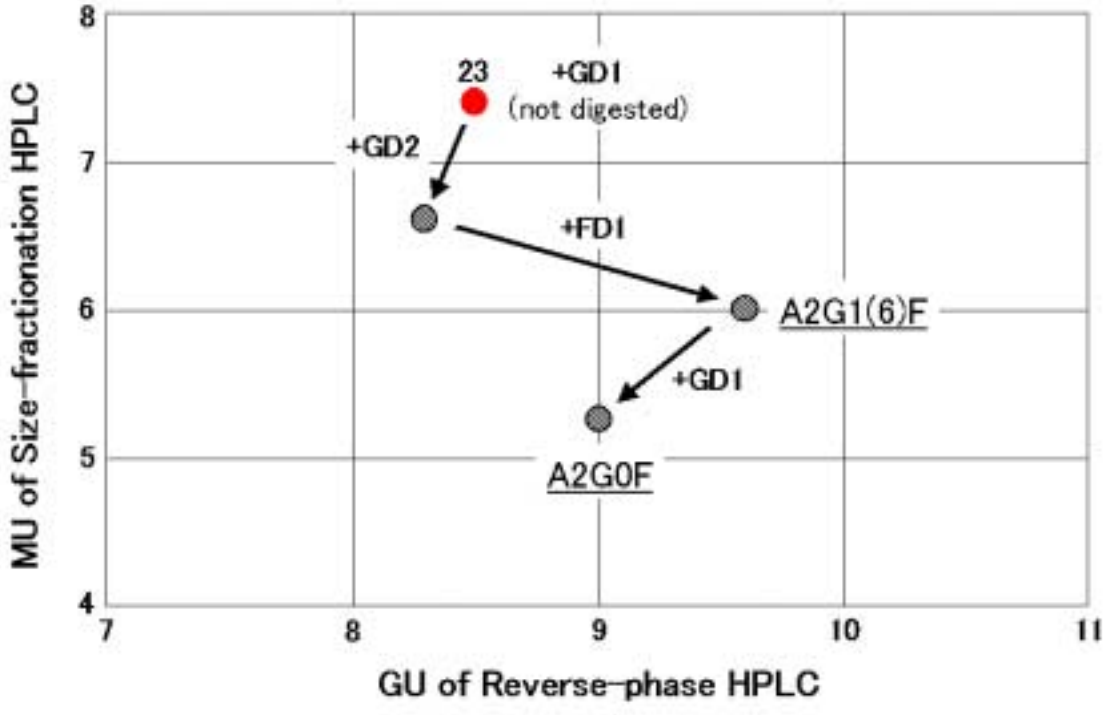
MU of Size-fractionation HPLC
GU of Reverse-phase HPLC
23
+GD1
(not digested)
+GD2
+FD1
A2G1(6)F
+GD1
A2G0F
8
7
6
5
4
7
8
9
10
11

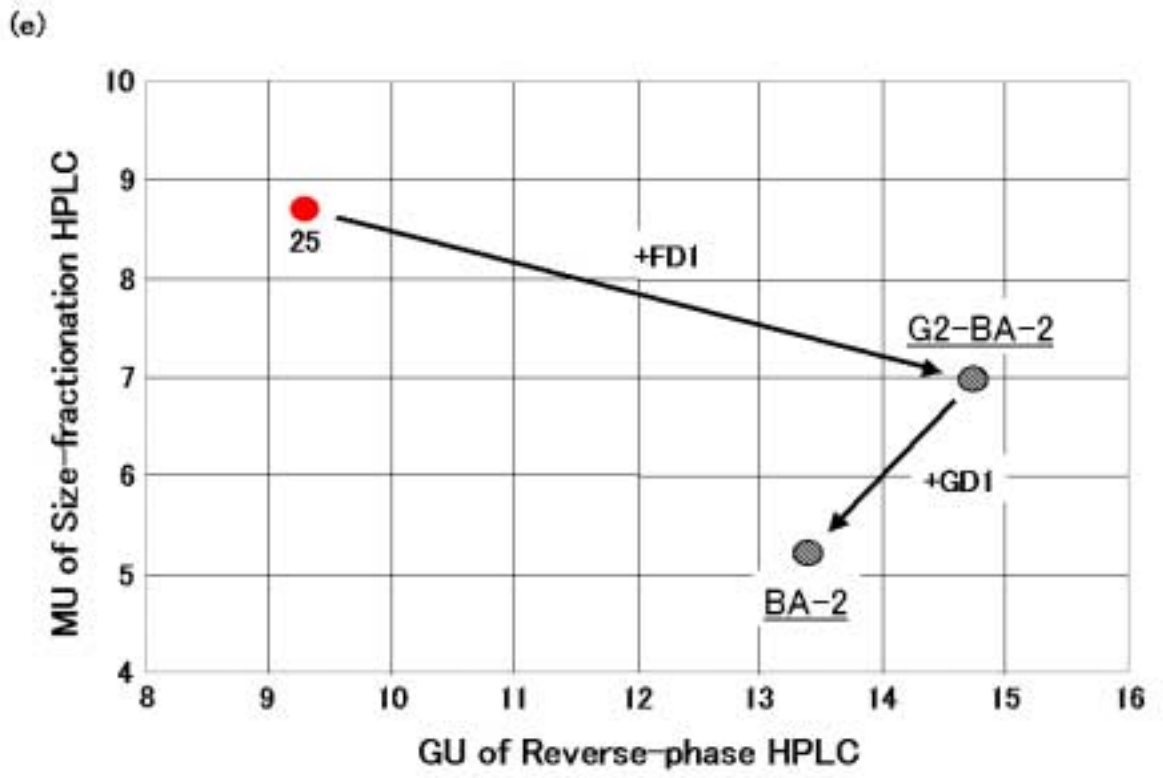

Fig. 4. *Identification of PA-sugar chain structures by exoglycosidase digestion combined with two-dimensional mapping.* The PA-sugar chains, (a) peak 8, (b) 23, (c) 25, (d) 22, (e) 18 and 19 (shown as red circles) were sequentially digested with several exoglycosidases until they matched on the two dimensional map to any standard PA-sugar chains commercially available (underlined the words), respectively. The abbreviations of the enzymes used in this study are described in Table 2. Note that the MU became smaller according to the rules when the monosaccharide residues were released with exoglycosidase digestion.

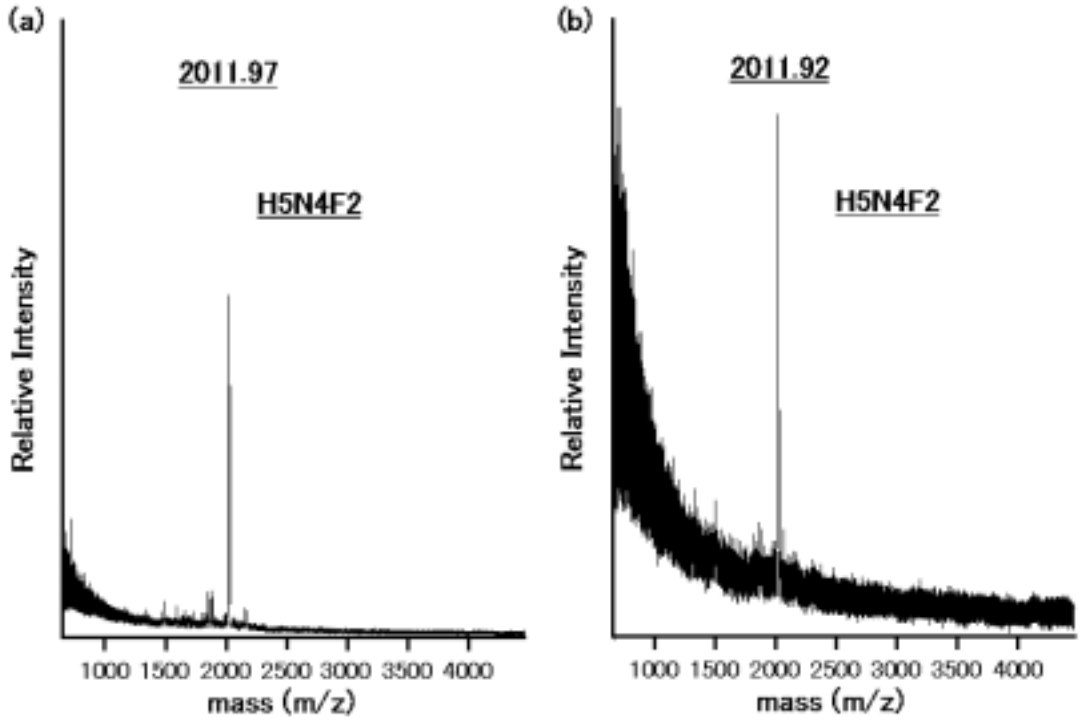

Fig. 5. *MALDI/TOF-MAS spectra of purified PA-sugar chains.* PA-sugar chains, peak 8 (a) and 23 (b) were pooled on size- or reverse-phase HPLC and their masses were acquired by MALDI/TOF-MAS. Masses shown are the monoisotopic mass of the MH^+ ions of the PA-sugar chains. The isobaric monosaccharide composition: H = hexose, N = N-acetylhexosamine, F = Fuc. Note that PA-sugar chains, peak 8 and 23 are different structure (see Table 1).

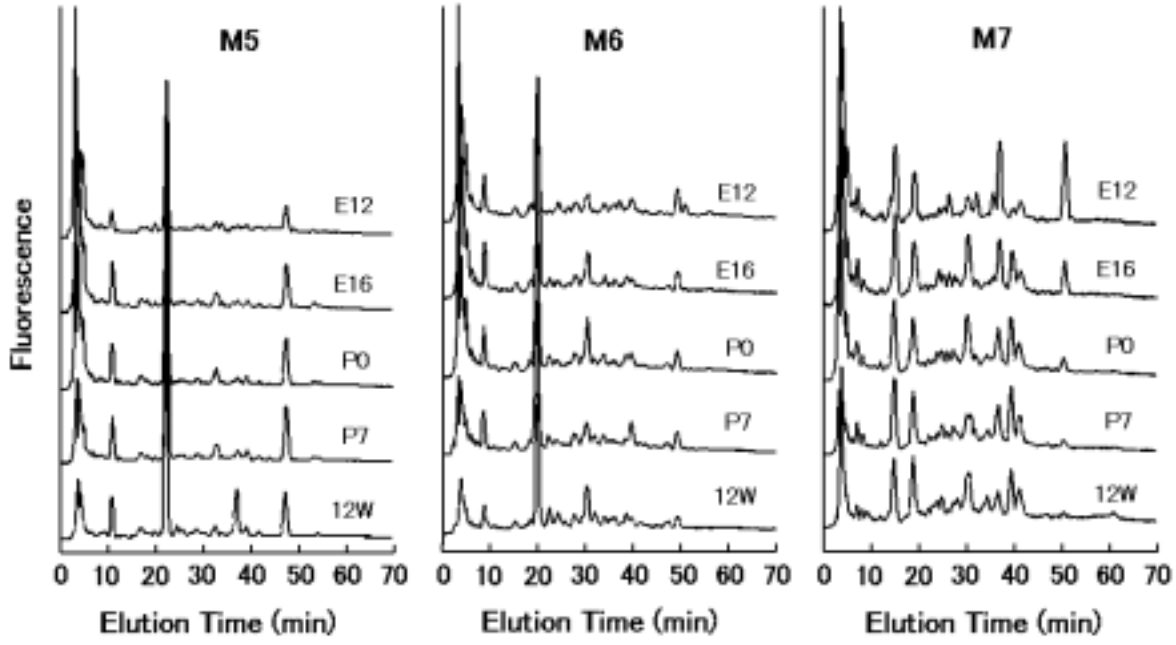

Fig. 6. *Elution profiles of N-linked sugar chains expressed in mouse cerebral cortex during development.* Representative three fractions (M5, M6 and M7) of reverse-phase HPLC from ICR mice cerebral cortex in difference ages (E12, E16, P0, P7 and 12 weeks) are shown.

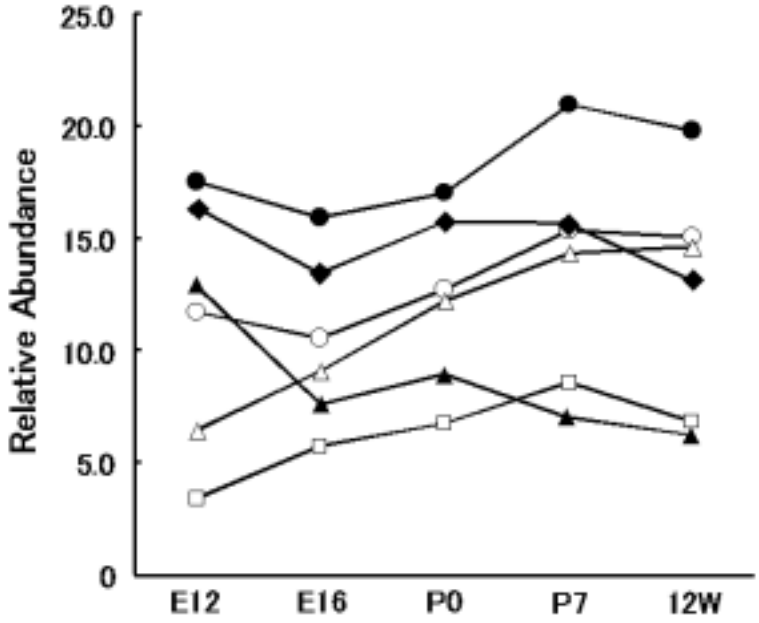

Fig. 7. *Structural features of N-linked sugar chains expressed in the cerebral cortex during development.* The relative abundance of N-linked sugar chains containing core Fuc (●), bisecting GlcNAc (○), β1-4Gal residues on the non-reducing ends (◆) with (□) and without outer-arm Fuc residues (▲) and GlcNAc residues on the non-reducing ends (△) is shown.

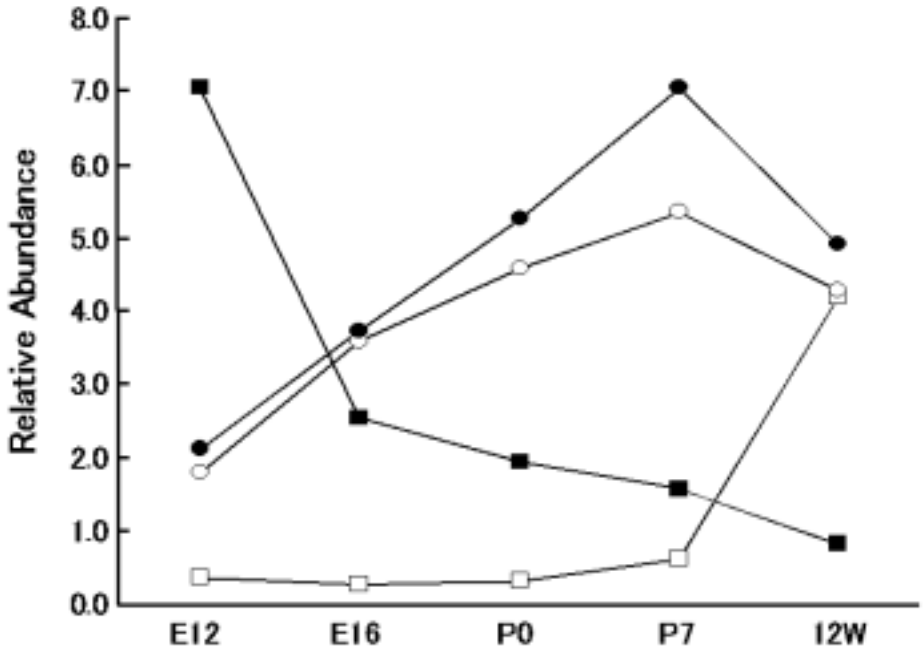

Fig. 8. *LewisX-BA-2 and BA-2 show similar expression profiles in the cerebral cortex during development.* Relative abundance value (RA) of BA-2 (○), BA-1 (□), Gal-BA-2 (■) and LewisX-BA-2 (●) from cerebral cortex is shown. The RA of Gal-BA-2 indicates the total of Ga-, Gb- and G2-BA2. The RA of LewisX-BA-2 indicates the total of LewisXa-, LewisXb and LewisX2-BA-2.

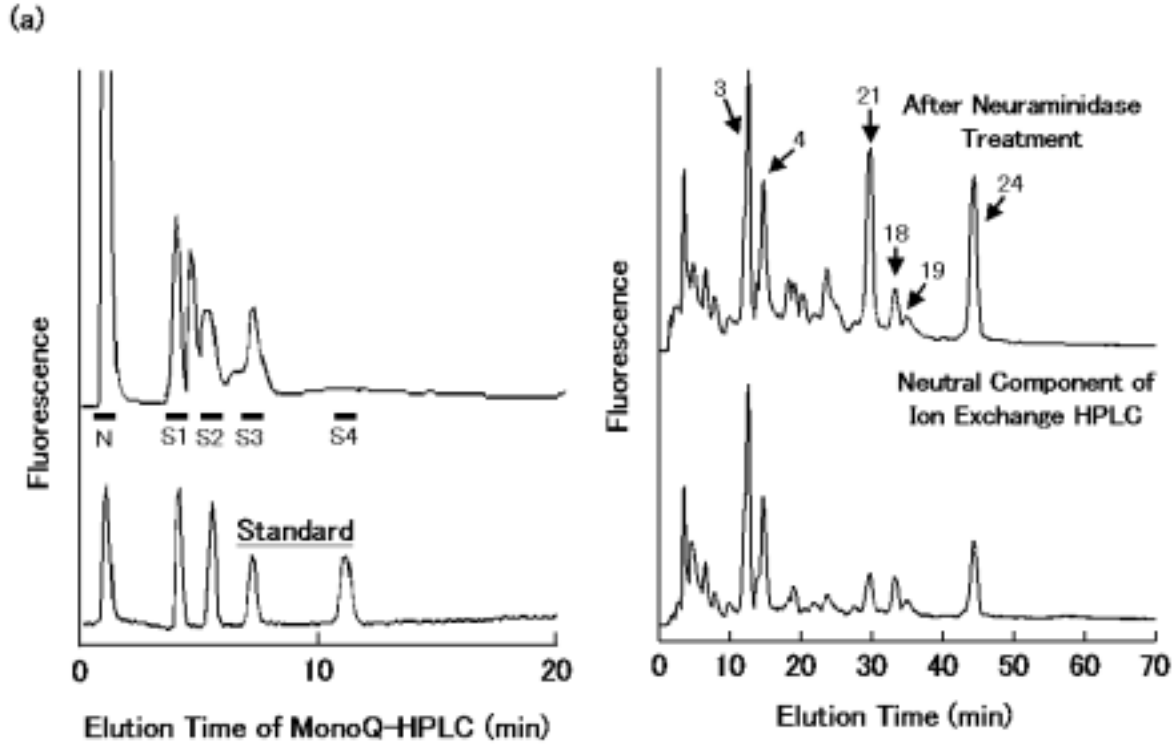
(a)
Fluorescence
N
S1
S2
S3
S4
Standard
0
10
20
Elution Time of MonoQ-HPLC (min)
3
4
21
18
19
24
After Neuraminidase Treatment
Neutral Component of Ion Exchange HPLC
0
10
20
30
40
50
60
70
Elution Time (min)

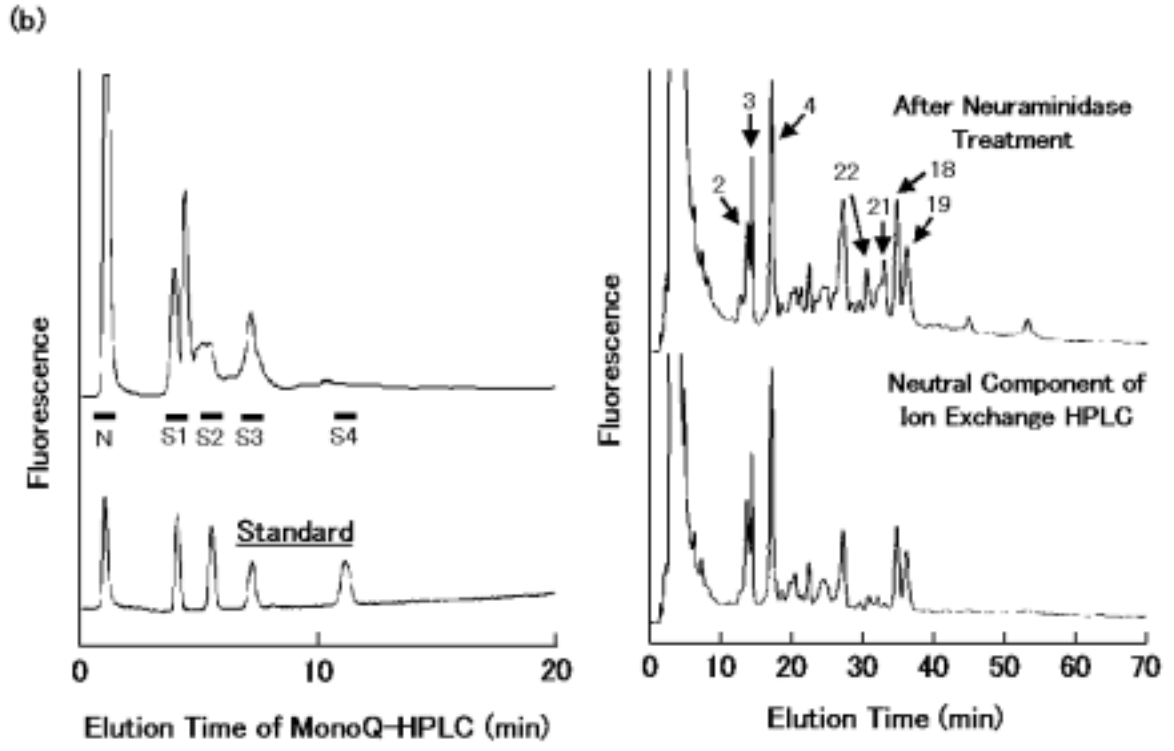
(b)
Fluorescence
N
S1
S2
S3
S4
Standard
0
10
20
Elution Time of MonoQ-HPLC (min)
2
3
4
22
21
18
19
After Neuraminidase Treatment
Neutral Component of Ion Exchange HPLC
0
10
20
30
40
50
60
70
Elution Time (min)

Fig. 9. *Most of LewisX-BA-2 is not sialylated in the cerebral cortex during development.* PA-sugar chains containing sialic acid (or negative charge) from E12 (a) and 12W (b) mice were purified with a Cellulose Cartridge Glycan preparation kit^{TM} and analyzed by ion exchange HPLC using a MonoQ HR5/5 column (left panel). PA-sugar chains were fractionated into the non-, mono-, di-, tri-, and tetra-sialylated components (N, S1-4) according to the N-acetyllactosamine type, biantennary standards. The N fraction and the neuraminidase-digested S1-S4 fractions were size fractionated and subjected to reverse-phase HPLC. M7 fraction of reverse-phase HPLC after neuraminidase treatments (right panel, upper) and fractionation of neutral component of ion exchange HPLC (right panel, lower) is shown. The peak numbers refers to the N-linked sugar chains in Table 1. Note that the peaks containing the partly or completely sialylated PA-sugar chains (#21, 22, 24) are lower in neutral component of ion exchange HPLC compared with those after neuraminidase treatment. The amounts of unsialylated PA-sugar chains, oligomannose series (#2, 3, 4), show no differences. There were no significant differences in the amounts of LewisXa- (#18) and LewisXb-BA-2 (#19) between the two different preparative methods (left panels, upper and lower). Furthermore, they were not detected in the neuraminidase-digested sialylated components (S1-4) in the two stages (data not shown).

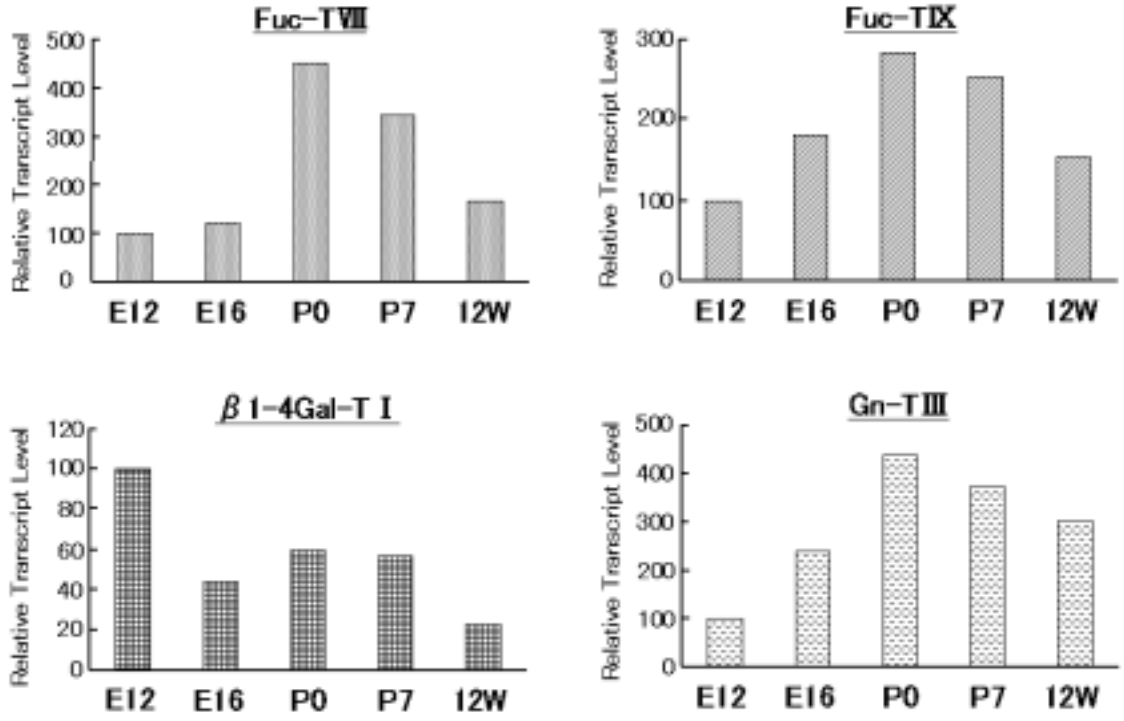

Figure. 10. *The developmental changes of glycosyltransferases mRNA expressions in mouse cerebral cortex.* Real-time RT-PCR analysis of the relative gene expressions of each glycosyltransferase was performed in mouse cerebral cortex of difference ages (E12, E16, P0, P7 and 12 weeks). The cDNA prepared from these samples was sequentially tested in LightCycler runs using mouse *Fuc-T Ⅷ*, *Fuc-TⅨ*, *β1-4Gal-T I*, *Gn-T Ⅲ* and *GAPDH* primers. In every run, a dilution series of E12 sample, as well as RT minus and water controls was included (although not shown here) and the standard curve was generated. Bars represent the relative transcript levels to that in E12 as 100, normalized to GAPDH mRNA transcript level.

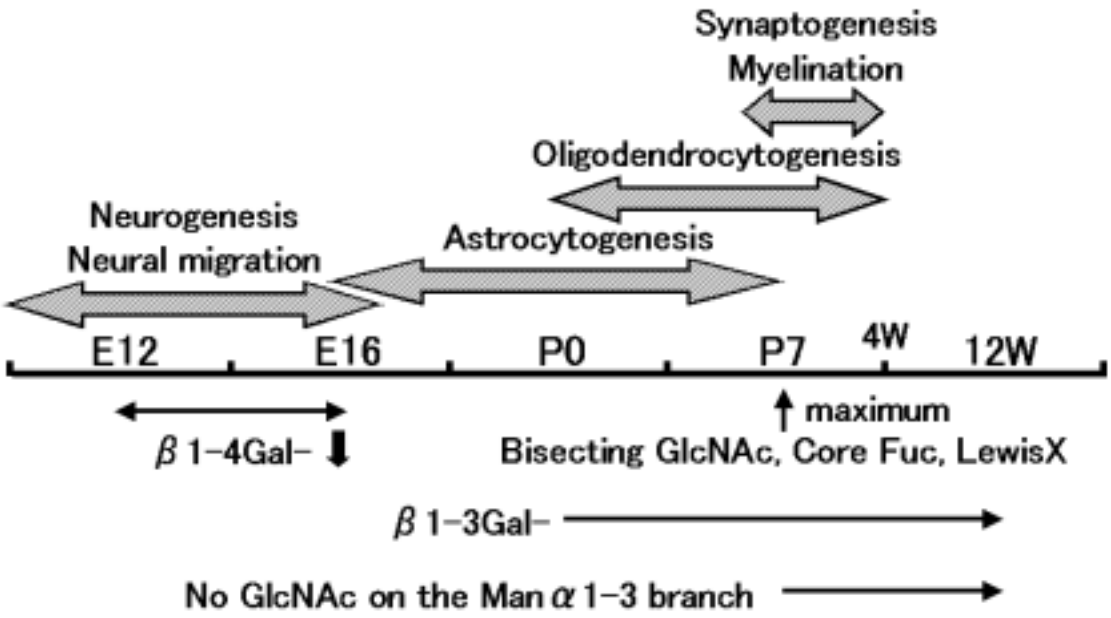

Figure. 11. *Diagram of the expression of brain-type N-linked sugar chains in the mouse cerebral cortex development.*

Table 1. *Structures and abbreviations of PA-sugar chains.*

Abbreviation (No.)	Structure
M9A (1)	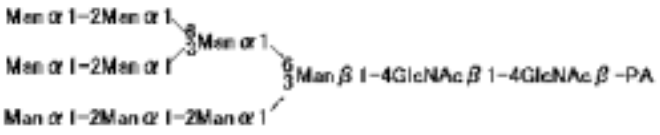
M8A (2)	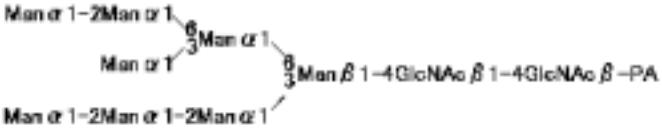
M7A (3)	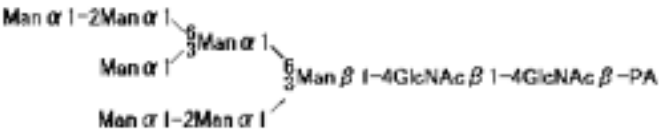
M7B (4)	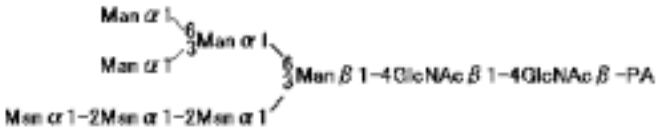
M6B (5)	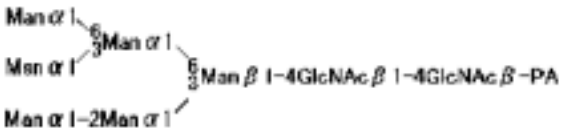
M5A (6)	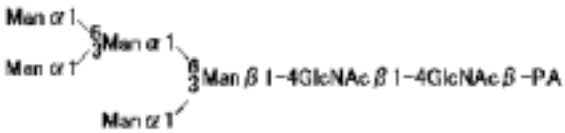
M4B (7)	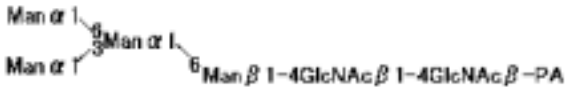

Abbreviation (No.)	Structure
LewisX-H4FB (8)	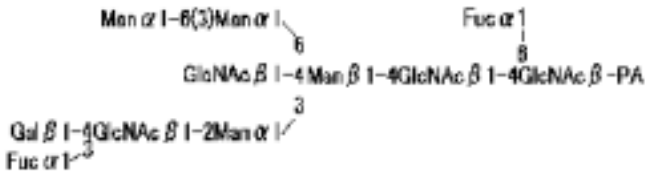
H5.1 (9)	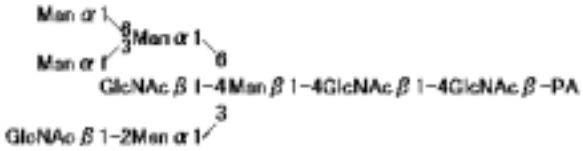
A0G0 (M3) (10)	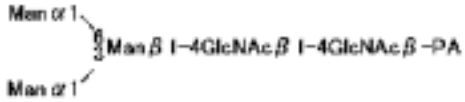
A0G0F (11)	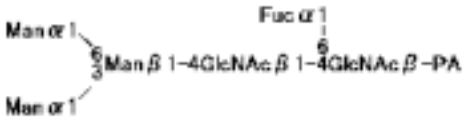
A1(6)G0F (12)	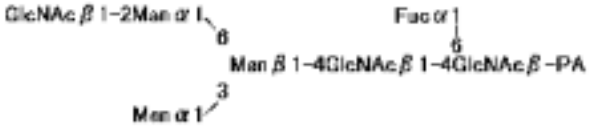
BA-1 (13)	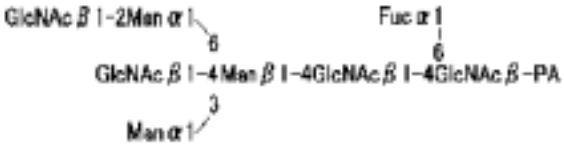
A2G0B (14)	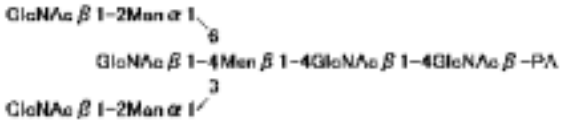

Abbreviation (No.)	Structure
A2G0F	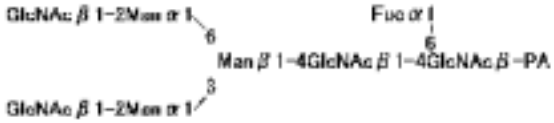
BA-2 (15)	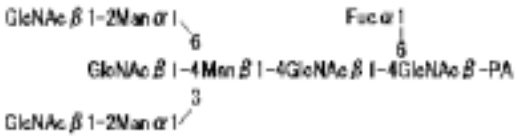
A2G1(6)F	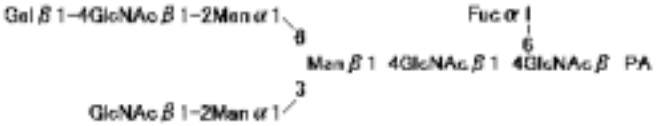
A2G1(3)F	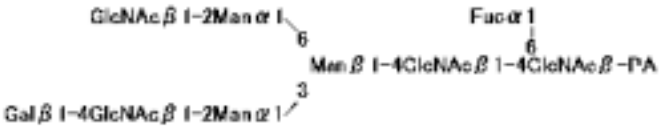
Ga-BA-2 (16)	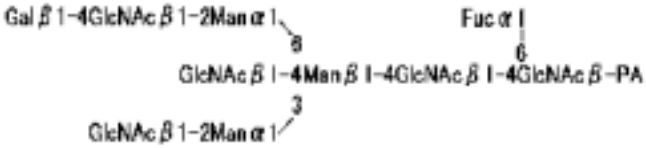
Gb-BA-2 (17)	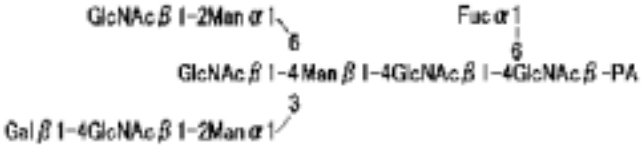
LewisXa-BA-2 (18)	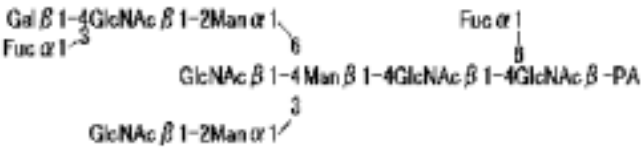

Abbreviation (No.)	Structure
LewisXb-BA-2 (19)	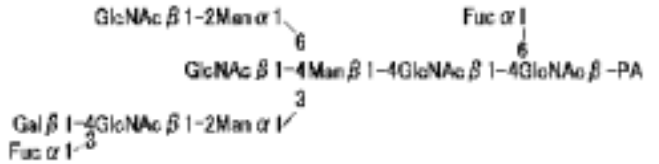
A2G2 (20)	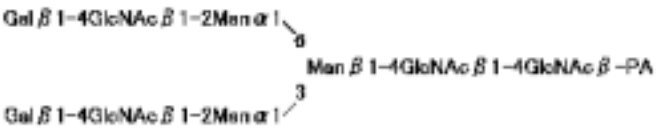
A2G2F (21)	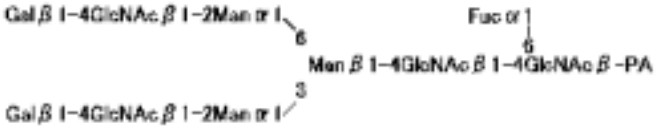
A2G'2F (22)	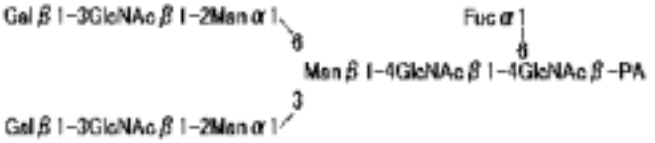
A2GFo(6)G'(3)F (23)	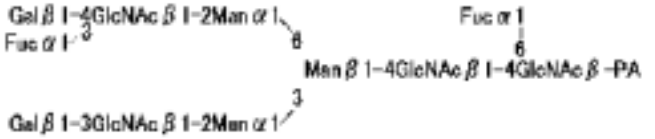
G2-BA-2 (24)	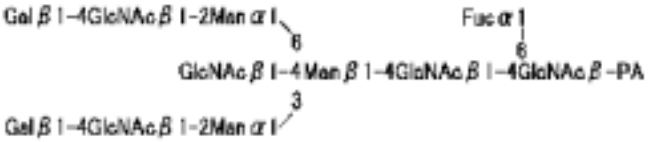
LewisX2-BA-2 (25)	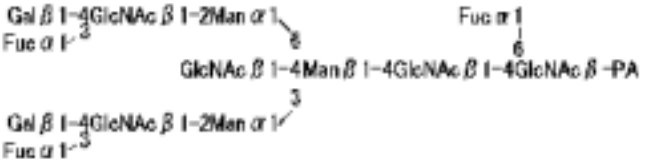

Table 2. *The substrate specificity of the exoglycosidases used in this study.*

Exoglycosidase	Spesificity
GD1: Diplococcus pneumoniae β-galactosidase (EC 3.2.1.23)	β(1,4)Gal
GD2: jack bean β-galactosidase (EC 3.2.1.23)	β(1,3/4)Gal
FD1: α1,3/4-L-fucosidase (Streptomyces sp.142, EC 3.2.1.51)	α(1,3/4)Fuc
FD2: bovine kidney α-fucosidase (EC 3.2.1.51)	α(1,6>1,2/3/4)Fuc
MD1: jack bean α-mannosidase (EC 3.2.1.24)	α(1,2/3/6)Man

Table 3. *Major N-linked sugar chains expressed in adult mouse brain.* The nomenclature of the structures is shown in "*Abbreviations*" and Table 1. RA values, relative abundance against total N-linked sugar chains from M3 to M11 fraction. $^{+}$PA-sugar chain masses were confirmed by MALDI/TOF-MAS as shown in Fig. 5.

No.	Abbreviation	RA	No.	Abbreviation	RA
1	M9A	5.5	14	A2G0B	0.9
2	M8A	3.9	15	BA-2	5.3
3	M7A	2.1	16	Ga-BA-2	0.5
4	M7B	2.1	17	Gb-BA-2	0.5
5	M6B	6.9	18	LewisXa-BA-2	2.0
6	M5A	20.5	19	LewisXb-BA-2	1.4
7	M4B	0.6	20	A2G2	3.4
8	LewisX-H4FB^{+}	1.1	21	A2G2F	1.6
9	H5.1	0.6	22	A2G'2F	0.9
10	A0G0	0.2	23	A2G1Fo(6)G'1(3)F^{+}	0.5
11	A0G0F	1.6	24	G2-BA-2	0.2
12	A1(6)G0F	0.3	25	LeiwsX2-BA-2	1.6
13	BA-1	4.2			

Table 4. *Expression of N-linked sugar chains is strictly regulated in mouse cerebral cortex.* N-linked sugar chains expressed in the cerebral cortices of five adult mice (a-e) are shown. The nomenclature of the structures is shown in the "*Abbreviations*" and Table 1. The values shown are the relative abundance against total N-linked sugar chains from M3 to M11 fraction.

No.	abbreviation	a	b	c	d	e	mean	SD
1	M9A	6.1	5.5	6.3	6.5	5.2	5.9	0.57
2	M8A	4.5	4.8	4.7	4.7	4.5	4.6	0.15
3	M7A	2.7	2.4	2.4	2.4	2.3	2.4	0.15
4	M7B	2.8	2.9	2.7	2.9	2.9	2.8	0.10
5	M6B	7.6	7.7	7.5	7.9	7.7	7.7	0.15
6	M5A	23.6	24.9	21.9	24.4	24.5	23.8	1.21
7	M4B	0.9	1.0	0.9	0.7	1.0	0.9	0.11
8	LewisX-H4FB	0.9	1.0	1.0	1.0	1.0	1.0	0.04
9	H5.1	0.6	0.6	0.6	0.6	0.6	0.6	0.03
10	A0G0	0.3	0.3	0.3	0.3	0.3	0.3	0.02
11	A0G0F	1.9	1.7	1.7	1.6	1.6	1.7	0.09
12	A1(6)G0F	0.2	0.2	0.3	0.3	0.3	0.3	0.02
13	BA-1	3.6	3.7	3.7	3.4	3.4	3.6	0.15
14	A2G0B	0.5	0.6	0.6	0.5	0.6	0.6	0.03
15	BA-2	4.6	4.5	4.3	3.9	4.4	4.3	0.25
16, 17	Ga+Gb-BA-2	0.6	0.6	0.7	0.5	0.6	0.6	0.09
18	LewisXa-BA-2	2.3	1.9	1.9	1.8	2.0	2.0	0.19
19	LewisXb-BA-2	1.4	1.2	1.1	1.2	1.2	1.2	0.10
20	A2G2	2.9	2.8	2.6	2.6	2.5	2.7	0.14
21	A2G2F	0.8	1.1	1.0	0.9	1.1	1.0	0.13
22	A2G'2F	0.4	0.5	0.6	0.4	0.4	0.5	0.07
23	A2G1Fo(6)G'1(3)F	0.4	0.5	0.4	0.4	0.4	0.4	0.02
24	G2-BA-2	0.0	0.1	0.1	0.1	0.1	0.1	0.06
25	LeiwsX2-BA-2	1.7	1.3	1.4	1.4	1.3	1.4	0.18

Table 5. *Major N-linked sugar chains expressed in developmental mouse cerebral cortex.* The nomenclature of the sugar chains is shown in "*Abbreviations*" and Table 1. The values shown are the relative abundances (RA) against total N-linked sugar chains from M3 to M11 fraction.

No.	abbreviation	E12	E16	P0	P7	12W	No.	abbreviation	E12	E16	P0	P7	12W
1	M9A	10.2	6.8	5.5	5.5	4.7	14	A2G0B	0.4	0.4	0.6	0.8	0.9
2	M8A	11.2	7.4	6.9	7.7	5.2	15	BA-2	1.8	3.6	4.6	5.3	4.3
3	M7A	3.8	2.9	3.0	3.1	2.0	16, 17	Ga+Gb-BA-2	2.2	1.2	1.4	1.3	0.7
4	M7B	2.6	1.9	2.1	2.9	2.5	18	LewisXa-BA-2	1.0	2.1	3.0	4.5	2.2
5	M6B	9.9	8.5	8.3	8.0	7.6	19	LewisXb-BA-2	0.4	0.8	1.3	1.1	1.5
6	M5A	7.6	12.4	14.7	16.8	23.5	20	A2G2	1.9	2.7	5.1	3.2	4.4
7	M4B	1.3	1.0	1.1	0.8	0.5	21	A2G2F	4.1	2.5	2.0	2.4	1.1
8	LewisX-H4FB	1.3	2.0	1.5	1.1	1.3	22	A2G'2F	0.0	0.0	0.4	1.1	0.8
9	H5.1	0.4	0.8	1.0	0.7	0.6	23	A2G1Fo(6)G'1(3)F	0.0	0.0	0.0	0.5	0.6
10	A0G0	0.7	0.8	0.1	0.4	0.3	24	G2-BA-2	4.9	1.4	0.6	0.3	0.1
11	A0G0F	0.9	1.3	1.1	1.4	1.5	25	LeiwsX2-BA-2	0.8	0.9	0.9	1.5	1.2
12	A1(6)G0F	0.0	0.0	0.0	0.0	0.3							
13	BA-1	0.3	0.3	0.3	0.6	4.2							